International Review of Financial Analysis 105 (2025) 104436

Contents lists available at ScienceDirect

International Review of Financial Analysis

journal homepage: www.elsevier.com/locate/irfa

On the limits of informationally efficient stock markets: New insights from a chartist-fundamentalist model ☆

Laura Gardini [a,b], Davide Radi [c,b], Noemi Schmitt [d], Iryna Sushko [c], Frank Westerhoff [d,*]

[a] Department of Economics, Society and Politics, University of Urbino Carlo Bo, Urbino, Italy
[b] Department of Finance, VSB-Technical University of Ostrava, Ostrava, Czech Republic
[c] DiMSEFA, Catholic University of the Sacred Heart, Milan, Italy
[d] Department of Economics, University of Bamberg, Bamberg, Germany

ARTICLE INFO

JEL classification:
C61
D84
G14

Keywords:
Market efficiency
Stock markets
Chartists and fundamentalists
Piecewise-linear discontinuous maps
Weird quasiperiodic attractors
Bifurcation analysis

ABSTRACT

We utilize a chartist-fundamentalist model to examine the limits of informationally efficient stock markets. In this model, chartists are permanently active in the stock market, while fundamentalists trade only when their mispricing-dependent trading signals are sufficiently strong. As a result, the model dynamics are driven by a two-dimensional piecewise-linear discontinuous map. Our findings suggest the possible coexistence of two distinct regimes. Depending on the initial conditions, the stock market may exhibit either constant or oscillatory mispricing. Constant mispricing occurs when chartists remain the sole active speculators, causing the stock price to converge toward a nonfundamental value. Conversely, the stock price oscillates around its fundamental value when fundamentalists repeatedly enter and exit the market. Interestingly, these oscillatory dynamics are associated with a new type of attractor, termed a "weird quasiperiodic attractor". When subjected to dynamic noise, our model reproduces several important stylized facts of stock markets and can thus be considered validated.

1. Introduction

The debate over whether stock markets are informationally efficient remains active among economists. Fama's (1970) "Efficient Market Hypothesis" asserts that stock markets are informationally efficient, meaning that stock prices reflect all available information. As a result, it is impossible to consistently achieve excess returns through technical or fundamental trading, as any new information that could impact prices is immediately and accurately incorporated into stock prices by rational market participants. In fact, Samuelson (1965) had already proven that informationally efficient stock prices are unforecastable and fluctuate randomly.

In contrast, Grossman and Stiglitz (1980) argue that if stock markets were perfectly efficient and stock prices always reflected all available information, there would be no incentive for speculators to gather and analyze information. Since information acquisition and analysis are costly activities, in a perfectly efficient market, the return on these activities would be negative because stock prices would already incorporate all information. This leads to a famous paradox: if no one gathers and analyzes information because it is unprofitable, then stock prices cannot fully reflect all available information, thereby contradicting the Efficient Market Hypothesis. Consequently, stock markets must exhibit some form of mispricing to compensate speculators for the costs incurred in acquiring and processing information. Somewhat ironically, Grossman and Stiglitz's (1980) framework reveals an equilibrium degree of disequilibrium, characterized by constant mispricing.

According to Farmer and Lo (1999), Lo (2004), and Farmer (2024), the "Adaptive Market Hypothesis" offers a more comprehensive and realistic evolutionary perspective on the informational efficiency of stock markets. Since speculators are boundedly rational, heterogeneous, and influenced by cognitive biases, their collective actions can result in mispricing. Nonetheless, speculators are capable of learning and adapting their trading behavior over time. Consequently, stock market mispricing is not constant, and market efficiency should be viewed as dynamic rather than static.

Given that the determinants of market efficiency remain unclear, we

☆ Presented at the 28th Workshop on Economics with Heterogeneous Interacting Agents, held from February 14 to 16, 2025, in Suzhou, China, and the 12th Workshop on Dynamic Models in Economics and Finance, held from September 12 to 14, 2024, in Urbino, Italy. We thank the participants, two anonymous referees, and the managing editor, Samuel Vigne, for their valuable feedback.

* Corresponding author at: University of Bamberg, Department of Economics, Feldkirchenstrasse 21, 96045 Bamberg, Germany.
E-mail address: frank.westerhoff@uni-bamberg.de (F. Westerhoff).

https://doi.org/10.1016/j.irfa.2025.104436
Received 31 October 2024; Received in revised form 11 April 2025; Accepted 24 June 2025
Available online 26 June 2025

propose a novel chartist-fundamentalist model to contribute to this important discussion. Our main findings are as follows. First, we identify conditions under which the stock price converges to a nonfundamental value, resulting in constant mispricing. Under the same conditions, oscillatory mispricing may also occur, characterized by the stock price fluctuating around its fundamental value. Coexisting attractors naturally integrate the insights of Grossman and Stiglitz (1980) and Farmer and Lo (1999) regarding the limits of informationally efficient stock markets within our model.[1] Second, the model's oscillatory mispricing is associated with a new type of attractor, termed a "weird quasiperiodic attractor". Third, by incorporating noise terms into the trading behavior of chartists and fundamentalists, we derive a stochastic version of our model that closely mimics the behavior of actual stock markets. Thus, our model can be considered empirically validated.

Recall that the chartist-fundamentalist approach, pioneered by Zeeman (1974), Beja and Goldman (1980), Day and Huang (1990), Lux (1995), and Brock and Hommes (1998), rests on the assumption that actual financial market participants rely on technical and fundamental analysis to predict stock prices. Menkhoff and Taylor (2007) and Hommes (2011) provide survey and experimental evidence supporting this assumption. As discussed by Murphy (1999), technical analysis seeks to derive trading signals from past stock price movements, a behavior often regarded as destabilizing. Fundamental analysis, reviewed by Graham and Dodd (1951), predicts that stock prices revert toward their fundamental values. Buying undervalued stocks and selling overvalued ones tends to stabilize stock market dynamics. Often, a market maker, who clears the market and adjusts the stock price in response to excess buying or selling, is included in these frameworks. This modeling device is also consistent with empirical evidence, see, e.g., Lillo, Farmer, and Mantegna (2003) and Bouchaud, Farmer, and Lillo (2009). Chartist-fundamentalist models reveal that interactions between speculators using technical and fundamental trading rules may trigger complex boom-bust dynamics in stock markets. For comprehensive literature reviews, see Hommes (2013), Dieci and He (2018), and Axtell and Farmer (2025).

Our model adheres to the empirically grounded core principles of the chartist-fundamentalist approach, and follows Farmer and Lo's (1999) perspective on how financial markets function. Specifically, a market maker quotes the stock price based on current excess demand, chartists extrapolate past price trends into the future, and fundamentalists speculate on mean reversion. Our point of departure is that fundamentalists abstain from trading when their risk-adjusted profit expectations become negative. This assumption reflects the main argument presented by Grossman and Stiglitz (1980): speculators need an incentive to gather and analyze fundamental information. In our model, fundamentalists follow their trading signals only when they are strong enough to promise sufficient profit for their risk-taking. When their trading signals are too weak, they become inactive, leaving the stock market to the chartists' trading behavior. Fundamentalists' band of inactivity is centered around the stock market's fundamental value, which, in turn, follows a random walk. We are interested in how closely the stock price will track its fundamental value.

In the absence of exogenous shocks, the stock price in our model is driven by a two-dimensional piecewise-linear discontinuous map that describes the two aforementioned constellations. Its dynamics depend on two parameters that measure the market impact of chartists and fundamentalists, allowing us to divide the corresponding parameter space into four distinct regions: R1, R2, R3, and R4. Broadly speaking, we observe the following results:

- In region R1, where the market impact of both chartists and fundamentalists is relatively low, the generic trajectory of the stock price always converges to a nonfundamental fixed point.
- In region R2, where the market impact of chartists and fundamentalists is moderate, the generic trajectory of the stock price either converges to a nonfundamental fixed point or exhibits endogenous dynamics.
- In region R3, where the market impact of fundamentalists is relatively high, the generic trajectory of the stock price either converges to a nonfundamental fixed point or displays divergent dynamics.
- In region R4, where the market impact of chartists is relatively high, the generic trajectory of the stock price is divergent.

The behavior of the stock market in regions R1 and R2 is of particular interest.

Consider region R1. Convergence to a nonfundamental fixed point implies constant mispricing. Since there is a continuum of fixed points within a band around the true fundamental value, the level of mispricing depends on the initial conditions. This convergence occurs because chartists are the only remaining speculators. As chartists do not receive trading signals prompting them to take a long or short position, the stock price remains unchanged. Although fundamentalists could theoretically trade on the mispricing, their expected risk-adjusted profits are negative. When the market impact of both chartists and fundamentalists is relatively low, this outcome represents the unique global behavior of our model.

In region R2, where the market impact of both is somewhat stronger but not too high, this regime may coexist with another regime that generates oscillatory stock market dynamics. Such dynamics arise from the interaction between chartists and fundamentalists, particularly from the repeated market entry and exit behavior of fundamentalists. For example, consider a scenario where the stock market is increasing but still quite undervalued. In this case, both chartists and fundamentalists receive a buy signal, and their joint trading behavior results in a strong price increase. This, in turn, lends the stock market significant momentum, causing the chartists' trading behavior to push the stock price considerably above its fundamental value. While fundamentalists may have temporarily exited the stock market, they now perceive profit opportunities and re-enter. As a result, the joint trading behavior of chartists and fundamentalists leads to a significant downswing.

We can analytically characterize the basins of attraction of the stock market's nonfundamental fixed points and the magnitude of the stock price fluctuations. Policymakers may use our findings to design more efficient stock markets. The boundaries of these basins of attraction and the extent of the stock price fluctuations depend, among other factors, on the market impact of chartists and fundamentalists, as well as the risk-adjusted profit expectations held by fundamentalists. Policymakers may influence these factors by implementing appropriate policies. This is particularly relevant, as such stock price dynamics occur under parameter settings that are typically associated with stable dynamics.

Erratic switches between low-volatility periods with relatively constant mispricing and more volatile stock price dynamics – during which the stock price oscillates around its fundamental value – occur in region R2 in the presence of fundamental shocks. Understanding the basins of attraction of the coexisting attractors is crucial for explaining such dynamic behaviors. Additionally, we find that a stochastic version of our model replicates key stylized facts of stock markets, including bubbles and crashes, excess volatility, fat-tailed return distributions, serially uncorrelated returns, and volatility outbursts.

A true highlight of our paper is the discovery of a new type of attractor, which we refer to as the "weird quasiperiodic attractor". These attractors are neither periodic nor chaotic; they represent something in between. The attracting sets we observe in our model appear quasiperiodic: the trajectory comes as close as desired to each point but never revisits any previous point, i.e., they are not periodic. By showing that our map does not possess repelling cycles, we can also exclude the

[1] We also find that stock prices may align with their fundamental values and evolve randomly, as envisioned by Fama (1970) and Samuelson (1965), although this occurs only under a very strict and unrealistic parameter configuration.

possibility that these attractors are chaotic. However, the global shape of the attractor is difficult to predict and its form is weird, justifying our terminology.[2] Notably, this type of attractor is reminiscent of "strange nonchaotic attractors" found in systems with quasiperiodic forcing, as described by Feudel, Kuznetsov, and Pikovsky (2006). However, strange nonchaotic attractors have fractal structures, motivating the term "strange". In contrast to "strange chaotic attractors", they do not display sensitivity to the initial conditions. Weird quasiperiodic attractors, in turn, emerge without any quasiperiodic forcing and it appears that they lack fractal structures.

The dynamics of our model are driven by a two-dimensional piecewise-linear discontinuous map. Such maps have recently been employed to study various phenomena in economics and finance, yielding several new insights. A key strength of these maps is their ability to provide clear-cut analytical insights into the functioning of economic systems, insights that are otherwise difficult to obtain. For studies using one-dimensional piecewise-linear maps, see Huang and Day (1993), Matsuyama (2007), Gardini, Sushko, and Naimzada (2008), Tramontana, Westerhoff, and Gardini (2010, 2013), Matsuyama, Sushko, and Gardini (2016) and Jungeilges, Maklakova, and Perevalova (2021, 2022). Two-dimensional piecewise-linear maps are explored by Anufriev, Gardini, and Radi (2020), Dieci, Gardini, and Westerhoff (2022), and Gardini, Radi, Schmitt, Sushko, and Westerhoff (2022, 2023, 2024). For general surveys on the dynamic properties of nonsmooth maps and their applications in the social and natural sciences, we refer readers to Zhusubaliyev and Mosekilde (2003), Puu and Sushko (2006), Di Bernardo, Budd, Champneys, and Kowalczyk (2008), and Avrutin, Gardini, Sushko, and Tramontana (2019).

We proceed as follows. Section 2 introduces our model. Sections 3 and 4 analyze its deterministic and stochastic dynamics, respectively. Section 5 concludes the paper. Appendices A and B provide proofs and additional discussions.

2. Model setup and law of motion

Our model highlights the trading behavior of a market maker and two types of speculators: chartists and fundamentalists. The market maker determines excess demand, clears the market by taking an offsetting long or short position, and sets the stock price for the next period. Chartists believe in the persistence of price trends, demanding stocks when prices rise and supplying stocks when prices fall. In contrast, fundamentalists believe in mean reversion, demanding stocks when the market is undervalued and supplying stocks when it is overvalued. Importantly, fundamentalists trade only when their risk-adjusted profit expectations are positive, which occurs when their trading signals are sufficiently strong. Otherwise, fundamentalists remain inactive, leaving the stock market driven solely by the trading behavior of chartists. The actions of both chartists and fundamentalists are influenced by noise, and the fundamental value of the stock market follows a random walk. Finally, there is a nonspeculative demand for stocks that matches the total supply of stocks.

2.1. Model setup

Let us detail our model's setup. Similar to Hommes, Huang, and Wang (2005), Dieci, Foroni, Gardini, and He (2006), and Westerhoff (2012), a market maker adjusts the log of the stock price based on current excess demand, using the log-linear price-adjustment rule

$$P_{t+1} = P_t + \alpha\left(D_t^C + D_t^F + D_t^R - N\right) \tag{1}$$

where α is a positive price adjustment parameter, and D_t^C and D_t^F represent the demands of chartists and fundamentalists. In addition, D_t^R denotes the nonspeculative (real) demand for stocks, and N is the total supply of stocks. Following Brock and Hommes (1998), we set the nonspeculative demand for stocks, representing the constant stock holdings of long-term investors, equal to the total supply of stocks, i.e.,

$$D_t^R = N \tag{2}$$

resulting in a zero net supply of outside stocks. Consequently, the market maker increases (decreases) the log of the stock price when speculators' demand for stocks exceeds (fall short of) their supply of stocks.

To determine their speculative investment positions in the stock market, chartists extrapolate past price trends into the future. See Murphy (1999) for a survey of technical trading rules. We formalize chartists' trading behavior as

$$D_t^C = \beta(P_t - P_{t-1}) + \chi_t \tag{3}$$

where β is a positive reaction parameter reflecting chartists' market impact with respect to their deterministic trading signals. Accordingly, chartists take long (short) positions in the stock market when the log of the stock price increases (decreases). Moreover, the random demand term $\chi_t \sim N(0, \sigma_\chi)$ captures the heterogeneity among chartists. See Brock and Hommes (1998), Franke and Westerhoff (2012), Scholl, Calinescu, and Farmer (2021), and Dieci et al. (2022) for related descriptions of the trading behavior of chartists.

Fundamentalists seek to exploit stock market mispricing, which is determined by the distance between the log of the stock price and the log of its fundamental value F_t. Generally, fundamentalists enter long positions when the stock market is undervalued and short positions when it is overvalued. See Graham and Dodd (1951) for a classical treatment of fundamental analysis. The trading behavior of fundamentalists is often formalized as $D_t^F = \gamma(F_t - P_t) + \phi_t$, where γ is a positive reaction parameter that captures the deterministic market impact of fundamentalists, and $\phi_t \sim N(0, \sigma_\phi)$ represents heterogeneity among them. See Brock and Hommes (1998), Franke and Westerhoff (2012), Scholl et al. (2021), and Gardini et al. (2022) for related examples.

However, as Grossman and Stiglitz (1980) argue, fundamentalists need an incentive to gather, analyze, and act on information. Given the complexity of determining an optimal market entry strategy, we assume that fundamentalists follow a simple rule of thumb, balancing the trade-off between expected profits and risk exposure. Specifically, fundamentalists abstain from the stock market when their expected risk-adjusted profits are negative. Let fundamentalists' expectations about the log of the stock price be given by $E_t^F[P_{t+1}] = P_t + \theta(F_t - P_t)$, with the expectation parameter $0 < \theta < 1$, so that they expect the log of the stock price to change by $E_t^F[\Delta P_{t+1}] = \theta(F_t - P_t)$. This expression approximates the gross return they anticipate. Fundamentalists consider two scenarios.

- First, when the stock market is undervalued, fundamentalists expect the stock price to rise and are willing to enter long positions. Their risk-adjusted profit expectations are given by $E_t^F[\pi_{t+1}] \approx E_t^F[\Delta P_{t+1}]\exp[P_t]D_t^F - \rho\exp[P_t]D_t^F$, where parameter $\rho > 0$ reflects their preference for risk compensation, which is proportional to their nominal investment positions in the stock market. Fundamentalists' expected risk-adjusted profits are positive if $F_t - P_t > \rho/\theta$.
- Second, when the stock market is overvalued, fundamentalists expect the stock price to decline and are willing to enter short positions. Their risk-adjusted profit expectations, now given by $E_t^F[\pi_{t+1}] \approx E_t^F[\Delta P_{t+1}]\exp[P_t]D_t^F + \rho\exp[P_t]D_t^F$, are positive if $F_t - P_t < -\rho/\theta$. To simplify the notation, let us define $h := \rho/\theta$.

[2] In two mathematical companion papers, Gardini, Radi, Schmitt, Sushko, and Westerhoff (2025a, 2025b) examine the properties of weird quasiperiodic attractors in greater detail.

Parameter h depends on fundamentalists' expectation formation behavior and risk attitudes.[3]

Combining these arguments, we formalize fundamentalists' trading behavior as

$$D_t^F = \begin{cases} \gamma(F_t - P_t) + \phi_t \text{ if } F_t - P_t > h \\ 0 \text{ if } -h \leq F_t - P_t \leq h \\ \gamma(F_t - P_t) + \phi_t \text{ if } F_t - P_t < -h \end{cases} \tag{4}$$

As before, parameter $\gamma > 0$ captures the deterministic market impact of fundamentalists, while the term $\phi_t \sim N(0, \sigma_\phi)$ represents their heterogeneity. The parameter h determines the critical level of the stock market's mispricing at which fundamentalists begin participating in trading. Clearly, fundamentalists act on their trading signals only when they are sufficiently strong, i.e., when they anticipate profits that adequately compensate for their risk exposure. When their trading signals are too weak, fundamentalists remain inactive.

We close our model by assuming that the log of the fundamental value of the stock market follows a random walk, specified as

$$F_{t+1} = F_t + \delta_t \tag{5}$$

where δ_t captures fundamental shocks, with $\delta_t \sim N(0, \sigma_\delta)$.

2.2. Law of motion of the model's deterministic skeleton

Let us derive the law of motion of the deterministic skeleton of our model. Setting $F_t = F$, $\chi_t = 0$, $\phi_t = 0$, and combining (1) to (4), it follows that the evolution of the log of the stock price in our model is governed by

$$P_{t+1} = \begin{cases} (1 + \alpha\beta - \alpha\gamma)P_t - \alpha\beta P_{t-1} + \alpha\gamma F \text{ if } P_t - F > h \\ (1 + \alpha\beta)P_t - \alpha\beta P_{t-1} \text{ if } -h \leq P_t - F \leq h \\ (1 + \alpha\beta - \alpha\gamma)P_t - \alpha\beta P_{t-1} + \alpha\gamma F \text{ if } P_t - F < -h \end{cases} \tag{6}$$

Since we are interested in how closely the log of the stock price tracks the log of its fundamental value, we define $x_t = P_t - F$. For ease of exposition, we also rename the aggregate parameters $\alpha\beta$ and $\alpha\gamma$ as b and c, respectively. From (5) and (6), we then obtain

$$x_{t+1} = \begin{cases} (1 + b - c)x_t - bx_{t-1} \text{ if } x_t > h \\ (1 + b)x_t - bx_{t-1} \text{ if } -h \leq x_t \leq h \\ (1 + b - c)x_t - bx_{t-1} \text{ if } x_t < -h \end{cases} \tag{7}$$

Moreover, introducing the auxiliary variable $y_t = x_{t-1}$ allows us to express the law of motion of the deterministic skeleton of our model in terms of the two-dimensional piecewise-linear discontinuous map

$$M : \begin{cases} x' = \begin{cases} f_R(x) = (1 + b - c)x - by \text{ if } x > h \\ f_M(x) = (1 + b)x - by \text{ if } -h \leq x \leq h \\ f_L(x) = (1 + b - c)x - by \text{ if } x < -h \end{cases} \\ y' = x \end{cases} \tag{8}$$

where the prime symbol stands for the unit time advancement operator. The branches $f_R(x)$ and $f_L(x)$ apply when chartists and fundamentalists are active, while $f_M(x)$ applies when fundamentalists abstain from the stock market.

Map M has the following properties. Recall that the parameters b, c, and h are positive. However, parameter h is a scaling factor. By changing variables to $x := x/h$ and $y := y/h$, we can set $h = 1$. In this sense, the dynamics of our model depend only on the parameters b and c, as well as the initial conditions x_0 and y_0. Nevertheless, due to its economic relevance, we retain parameter h in our computations. Since $M(-x, -y) = -M(x, y)$, the map M is symmetric with respect to the origin. Therefore, any invariant set of map M is either symmetric with respect to the origin or has a corresponding set symmetric with respect to the origin. See Appendix B for further discussion.

3. Deterministic model dynamics

3.1. Preliminary observations

Before proceeding with the analysis of map M, let us investigate two special cases. For $h = \infty$, map M becomes map

$$C : \begin{cases} x' = (1 + b)x - by \\ y' = x \end{cases} \tag{9}$$

Map C describes the deterministic dynamics of the log of the stock price in deviation from the log of its fundamental value when chartists are the sole type of active speculator. For $h = 0$, map M reduces to map

$$F : \begin{cases} x' = (1 + b - c)x - by \\ y' = x \end{cases} \tag{10}$$

Map F captures the deterministic dynamics of the log of the stock price in deviation from the log of its fundamental value when chartists and fundamentalists are always jointly active.

What can we conclude about maps C and F? Let us start with map F. Map F has a unique fixed point at the origin. At this so-called fundamental fixed point, the stock market is informationally efficient, meaning that the stock price equals its fundamental value. The Jacobian matrix of map F reads

$$J_F = \begin{bmatrix} 1 + b - c & -b \\ 1 & 0 \end{bmatrix} \tag{11}$$

with trace $tr = 1 + b - c$ and determinant $det = b$. The eigenvalues of the matrix are $\lambda_{1,2} = \left(1 + b - c \pm \sqrt{(1 + b - c)^2 - 4b}\right)/2$. These eigenvalues lie inside the unit circle, implying that the fixed point of map F is globally stable, provided the following stability conditions are jointly satisfied: (i) $1 + tr + det > 0$, (ii) $1 - tr + det > 0$, and (iii) $1 - det > 0$. As can be easily verified, the stability domain of the fixed point of map F is defined by the stability box S, given as $0 < c < 2 + 2b$ and $0 < b < 1$. The stability box S is depicted in green in the left panel of Fig. 1. Within this stability box, the eigenvalues fall into three sub-regions: S1, S2, and S3, where the eigenvalues are complex conjugate, real and negative, and real and positive, respectively. Outside the stability box, in the gray region, the dynamics are divergent.

The left panels of Fig. 2 presents three examples of the dynamics of map F in the time domain. The pink lines depict x_t and the green lines $x = 0$. The right panels show the corresponding behavior in state space, with the 45-degree lines marked in blue. We will clarify the meaning of the black lines in the sequel. The parameter setting in the top panels is $b = 0.80$ and $c = 1.35$. Since this parameter combination is located in sub-region S1, the log of the stock price in deviation from the log of its fundamental value displays dampened oscillations around its fundamental fixed point. The parameter setting in the middle panels, $b = 0.20$ and $c = 2.30$, is located in sub-region S2, resulting in an alternating adjustment path. The parameter setting in the bottom panels, $b = 0.20$ and $c = 0.30$, is located in sub-region S3, yielding a monotonic adjustment path.

To summarize the main implications of map F, as long as the reaction parameters of chartists and fundamentalists remain within the stability box S, their joint trading behavior eventually leads to informationally efficient stock markets. In other words, mispricing is only a temporary phenomenon. According to Fama (1970), the stock price always reflects its fundamental value. For the parameter configuration $b = 0$ and $c = 1$, the log of the stock price consistently equals the log of its fundamental value. If the log of the fundamental value follows a random walk, then

[3] Future work could explore more sophisticated market entry rules. For instance, it would be interesting to examine the effects of asymmetric market entry levels. Moreover, parameter θ may also reflect trading costs that are proportional to fundamentalists' positions in the market.

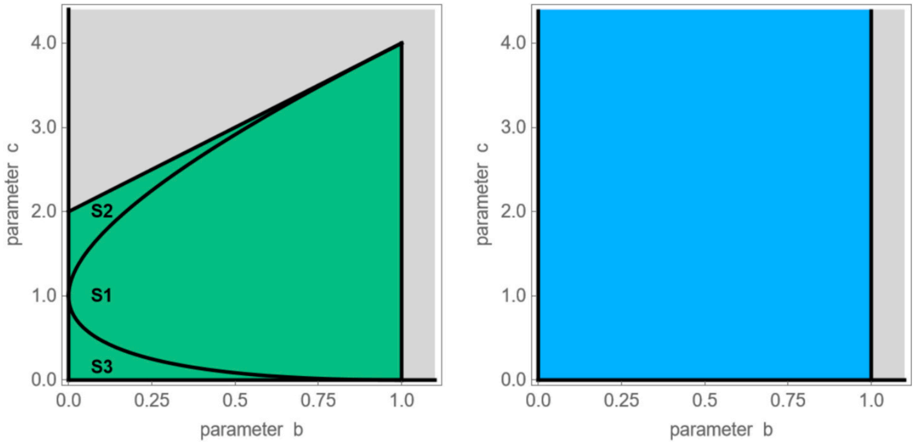

Fig. 1. Stability domains of the fixed points of maps F and C. The green region in the left panel represents the stability domain of the unique fixed point of map F. In sub-regions S1, S2, and S3, the eigenvalues are complex conjugate, real and negative, and real and positive, respectively. The blue region in the right panel represents the stability domain of the continuum of fixed points of map C. Parameter combinations shown in gray correspond to divergent dynamics. (For interpretation of the references to colour in this figure legend, the reader is referred to the web version of this article.)

the log of the stock price does as well – consistent with Samuelson's (1965) prediction that informationally efficient stock prices fluctuate randomly. However, this outcome relies on a strict and, given that it ignores the market impact of chartists, unrealistic parameter assumption.

Map C has a continuum of fixed points, corresponding to the entire 45-degree line. At these so-called nonfundamental fixed points, the stock market is mispriced, except at the origin. The Jacobian matrix of map C is

$$J_C = \begin{bmatrix} 1+b & b \\ 1 & 0 \end{bmatrix} \tag{12}$$

with trace $tr = 1 + b$ and determinant $det = b$. Its two eigenvalues are $\lambda_1 = 1$ and $\lambda_2 = b$. The general solution of map C is given by

$$G = \begin{cases} x_t = \dfrac{by_0 \quad x_0}{b \quad 1} \quad \dfrac{b\ y_0 \quad x_0)}{b \quad 1} b^t \\ y_t = \dfrac{by_0 \quad x_0}{b \quad 1} \quad \dfrac{b\ y_0 \quad x_0)}{b \quad 1} b^{t \quad 1} \end{cases} \tag{13}$$

Starting from the initial conditions (x_0,y_0), the system ultimately converges to the fixed point $\left(\frac{by_0 \quad x_0}{b \quad 1}, \frac{by_0 \quad x_0}{b \quad 1}\right)$, as long as $0 < b < 1$. In state space, the dynamics of map C evolve along the line $y = \frac{x}{b} + \frac{by_0 \quad x_0}{b}$. The blue region in the right panel of Fig. 1 shows the stability domain of the continuum of fixed points of map C. For $b > 1$, the dynamics are divergent. This parameter region is depicted in gray.

Fig. 3, based on $b = 0.80$, presents two examples of the dynamics of map C, using the same design as Fig. 2. For the initial conditions (0.13, 0.17), the log of the stock price in deviation from the log of its fundamental value moves toward the nonfundamental fixed point (0.03, 0.03). For the initial conditions (0.10, 0.17), the log of the stock price in deviation from the log of its fundamental value reaches the nonfundamental fixed point (0.18,0.18). Apparently, the stock market's final mispricing hinges on the initial conditions.

To summarize the main implications of map C, as long as $0 < b < 1$, all the initial conditions yield constant mispricing, except for those located on the line $y = x/b$. However, the final mispricing may be quite substantial, and in such cases, we would expect fundamentalists to seek to exploit it.

In fact, our focus is not on the isolated dynamics of maps F and C, but rather on their joint dynamics, represented by map M. In Figs. 2 and 3, the black vertical and horizontal lines indicate the parameter h, set to $h = 0.05$. According to our model, fundamentalists are inactive if $h \leq x \leq h$. As a result, certain dynamics observed in Figs. 2 and 3 are not compatible with map M. The dynamics of map F are valid outside the black lines, while the dynamics of map C are valid inside them. In the examples depicted in Figs. 2 and 3, these boundaries are violated. With these insights in hand, we are now prepared to examine map M.

Map M has three branches, namely $f_L(x)$, $f_M(x)$, and $f_R(x)$. Their regions of definition are shown in the left panel of Fig. 4 for $h = 0.05$. Due to its outer branches $f_R(x)$ and $f_L(x)$, map M has two fixed points with identical coordinates at the origin. However, these fundamental fixed points are virtual since they exist outside the regions where their respective branches are defined. The Jacobian matrices of the branches $f_R(x)$ and $f_L(x)$ of map M are identical to that of map F, i.e., $J_F = J_R = J_L$. In addition, due to its inner branch $f_M(x)$, map M has a continuum of real fixed points with $h \leq x = y \leq h$, represented by segment S^*. Only one of these fixed points, the origin, ensures informationally efficient stock markets. All other nonfundamental fixed points on segment S^* result in constant mispricing. In the left panel of Fig. 4, the segment S^* of fixed points is marked in blue, with the origin highlighted in green. The remaining points on the 45-degree line (blue dots) are virtual fixed points of branch $f_M(x)$ of map M. In contrast to map C, steady-state mispricing is now bounded, with its maximal level determined by parameter h. This is ensured by the market entry behavior of fundamentalists. The Jacobian matrix of branch $f_M(x)$ of map M is identical to that of map C, i.e., $J_C = J_M$.

What might the dynamics of map M look like? Fig. 5, based on $b = 0.80$, $c = 2.50$, and $h = 0.05$, presents two examples. The left (right) panels portray the dynamics in the time domain (state space). The first example starts with the initial conditions $x_0 = \quad 0.12$ and $y_0 = \quad 0.16$. After a few time steps, the log of the stock price in deviation from the log of its fundamental value has converged to one of the nonfundamental fixed points of map M, yielding constant mispricing. From now on, we will depict such fixed-point dynamics in blue. The second example rests on the initial conditions $x_0 = 0.13$ and $y_0 = 0.00$. Here, the log of the stock price in deviation from the log of its fundamental value exhibits endogenous dynamics, an outcome that we will now always report in red. While mispricing is bounded, it oscillates, giving rise to a weird quasiperiodic attractor.[4] Obviously, the initial conditions matter.

To explore the dependence of our model's dynamics on the initial

[4] Gardini, Radi, Schmitt, Sushko, and Westerhoff (2025c) show that the emergence of weird quasiperiodic attractors does not hinge on the assumption that all fundamentalists are risk averse, respectively, that map M possesses a continuum of nonfundamental fixed points.

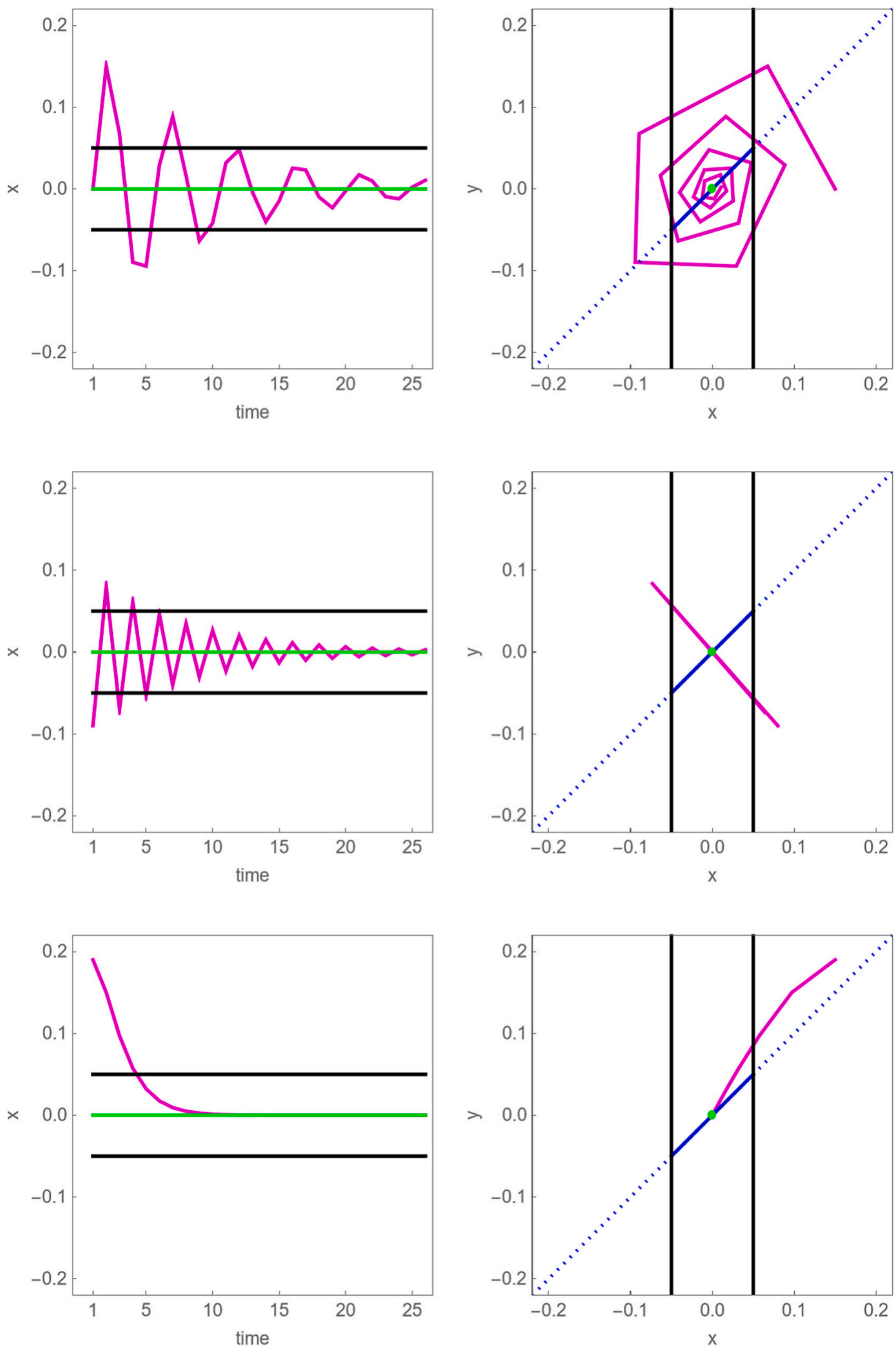

Fig. 2. Dynamics of map F. The pink, green, and black lines in the left panels depict x_t, $x = 0$ and $x = \pm h$, respectively. The right panels show the corresponding behavior in state space, with the 45-degree lines marked in blue. Top: $b = 0.80$, $c = 1.35$, $x_0 = 0.15$, and $y_0 = 0.00$. Middle: $b = 0.20$, $c = 2.30$, $x_0 = 0.08$, and $y_0 = 0.09$. Bottom: $b = 0.20$, $c = 0.30$, $x_0 = 0.15$, and $y_0 = 0.19$. (For interpretation of the references to colour in this figure legend, the reader is referred to the web version of this article.)

conditions in more detail, we visualize the basins of attraction of map M's coexisting attractors in the right panel of Fig. 4. Computations of basins of attraction in our paper are consistently conducted using a 250 by 250 grid. Here, the initial conditions are varied in the intervals $0.20 < x < 0.20$ and $0.20 < y < 0.20$. The basin of attraction of the segment S^* of fixed points is marked in light blue, while all other initial conditions, represented in light red, converge to a weird quasiperiodic attractor, depicted in red. Weird quasiperiodic attractors are a completely new dynamical phenomenon, which we study in more detail in the sequel.

The dynamics of our model naturally depend on the underlying parameter settings. To broaden our perspective, Fig. 6 presents two-dimensional bifurcation diagrams using a 250 by 250 grid, where we vary parameters b and c within the ranges $0.00 < b < 1.10$ and $0.00 < c < 4.40$, while setting parameter h to $h = 0.05$. In the left panel, the initial conditions are $x_0 = 0.06$ and $y_0 = 0.06$. Green dots indicate convergence to the fundamental fixed points, blue dots represent convergence to a nonfundamental fixed points, red dots imply endogenous dynamics, and gray dots reflect divergent dynamics. Notably, no green dots are present – none of the simulations resulted in convergence

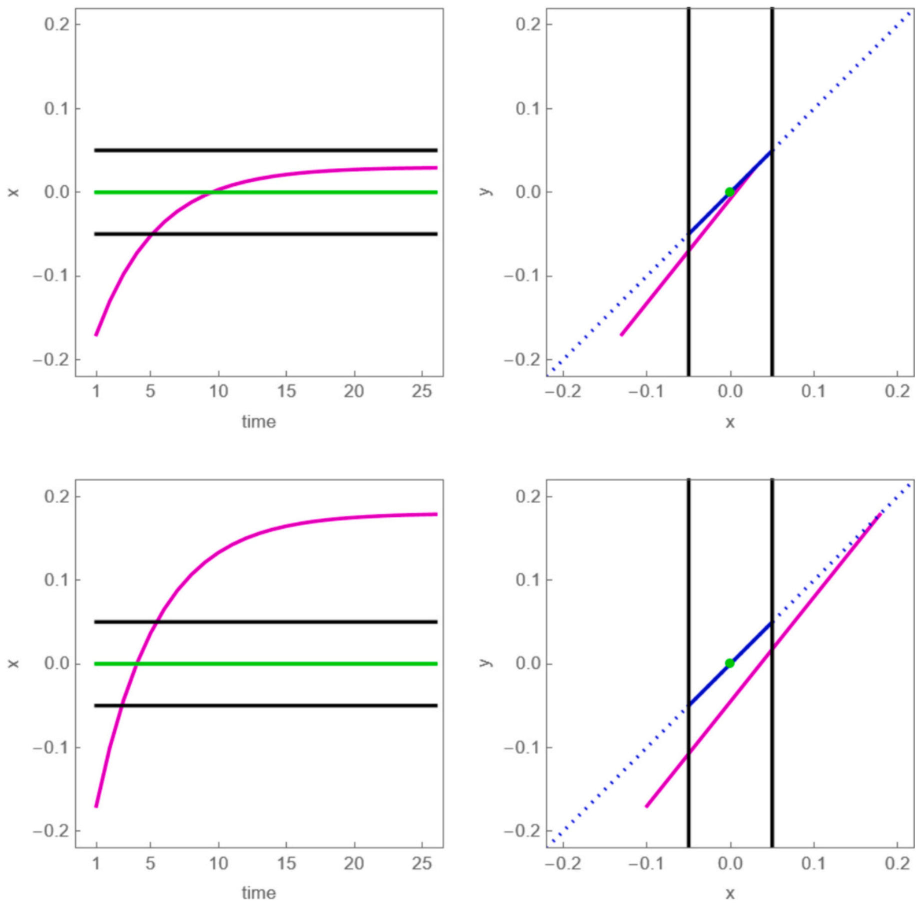

Fig. 3. Dynamics of map C. The pink, green, and black lines in the left panels depict x_t, $x = 0$ and $x = \pm h$, respectively. The right panels show the corresponding behavior in state space, with the 45-degree lines marked in blue. Top: $b = 0.80$, $x_0 =$ 0.13, and $y_0 =$ 0.17. Bottom: $b = 0.80$, $x_0 =$ 0.10, and $y_0 =$ 0.17. (For interpretation of the references to colour in this figure legend, the reader is referred to the web version of this article.)

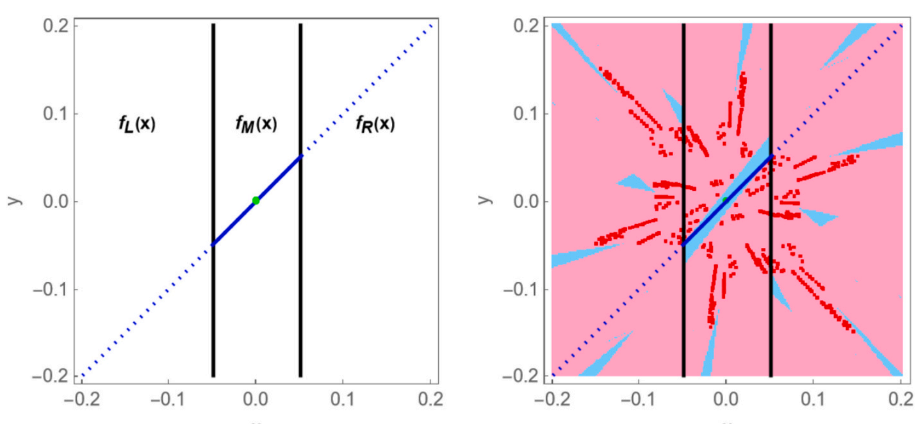

Fig. 4. Properties of map M. The left panel shows the regions of definition for the branches $f_L(x)$, $f_M(x)$, and $f_R(x)$ of map M. The segment S^* of fixed points and the origin are depicted in blue and green, respectively. The right panel shows the basin of attraction of the segment S^* of fixed points in light blue. The initial conditions marked in light red converge to a weird quasiperiodic attractor, represented by the red dots. Parameter setting: $b = 0.80$, $c = 2.50$, and $h = 0.05$. (For interpretation of the references to colour in this figure legend, the reader is referred to the web version of this article.)

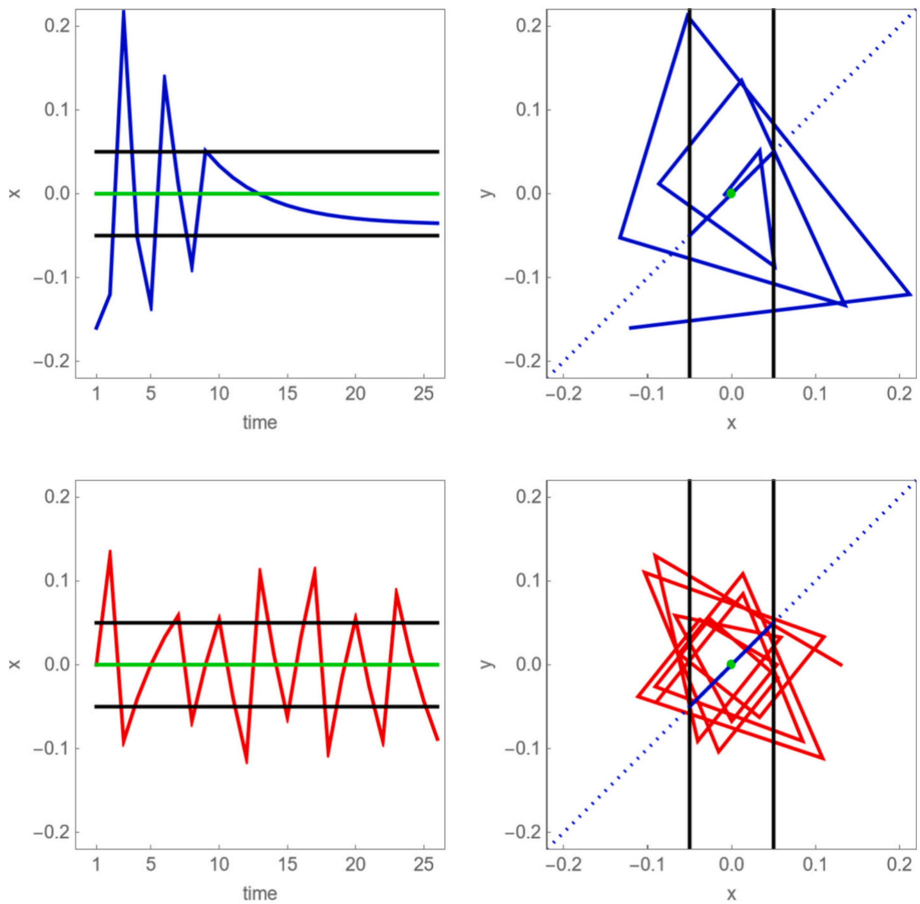

Fig. 5. Dynamics of map M for $b = 0.80$, $c = 1.35$, and $h = 0.05$. The blue, red, green, and black lines in the left panels depict the fixed-points dynamics of x_t, the weird-quasiperiodic dynamics of x_t, $x = 0$, and $x = \pm h$, respectively. The right panels show the corresponding behavior in state space, with the 45-degree lines marked in blue. Initial conditions: $x_0 =$ 0.12 and $y_0 =$ 0.16 (top) and $x_0 = 0.13$ and $y_0 = 0.00$ (bottom). (For interpretation of the references to colour in this figure legend, the reader is referred to the web version of this article.)

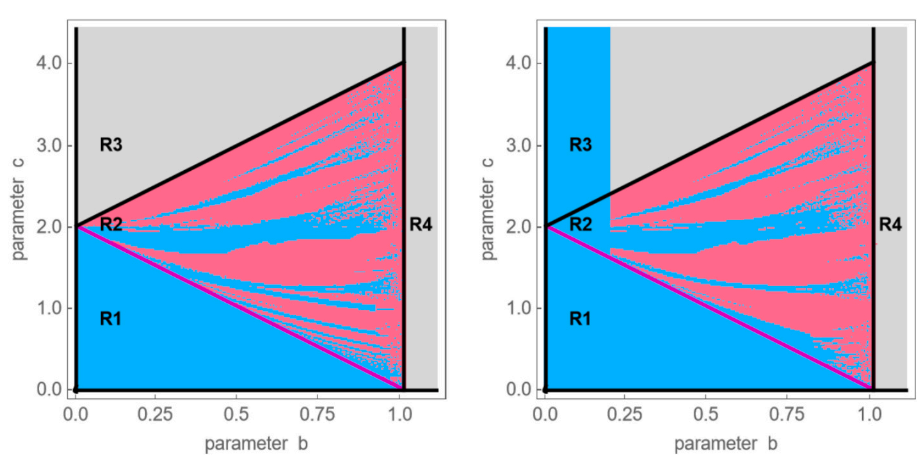

Fig. 6. Two-dimensional bifurcation diagrams for map M. Parameters b and c are varied between $0.00 < b < 1.10$ and $0.00 < c < 4.40$, while parameter h is set to $h = 0.05$. Initial conditions: $x_0 = 0.06$ and $y_0 = 0.06$ (left) and $x_0 = 0.04$ and $y_0 = 0.00$ (right). Blue dots: fixed-point dynamics. Red dots: weird-quasiperiodic dynamics. Gray dots: divergent dynamics. See Proposition 2 for an explanation of sub-regions R1, R2, R3, and R4. (For interpretation of the references to colour in this figure legend, the reader is referred to the web version of this article.)

to the fundamental fixed points. The right panel repeats this exercise with the initial conditions $x_0 = 0.04$ and $y_0 = 0.00$. For low values of parameter b, previously divergent dynamics transition into fixed-point dynamics. Our model therefore contradicts Fama's (1970) claim that financial markets are informationally efficient.

It is insightful to compare these numerically generated findings with those reported in Fig. 1. The parameter space appears to be divided into four sub-regions, displaying (1) convergence to a nonfundamental fixed point, (2) convergence to a nonfundamental fixed point or the emergence of endogenous dynamics, (3) convergence to a nonfundamental fixed point or divergent dynamics, and (4) divergent dynamics. Apart from the magenta line, the boundaries of these regions are already visible in Fig. 1. The next section reveals that we can rigorously prove this hypothesis, identify the magenta boundary, characterize the basins of attraction of the coexisting attractors, and formally establish the appearance of weird quasiperiodic attractors.

3.2. Main analytical results

Propositions 1 and 2, proven in Appendix A, present our main

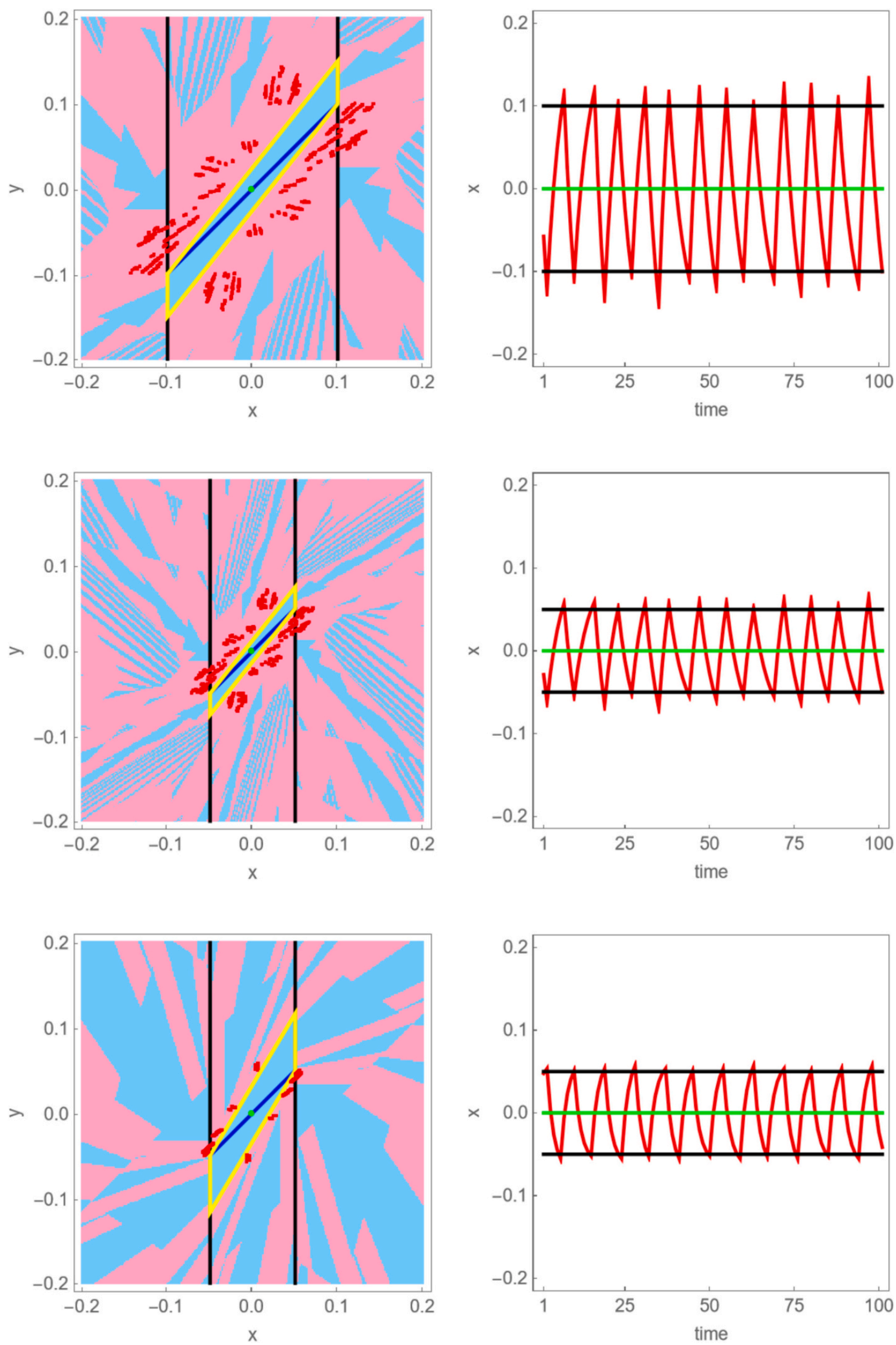

Fig. 7. Immediate basin of attraction of the segment S^* of fixed points. Left: The boundaries of the immediate basin of attraction of the segment S^* of fixed points are marked in yellow. The segment S^* of fixed points is represented in blue, and the origin is shown in green. The initial conditions, depicted in light blue and light red, converge to nonfundamental fixed points and a weird quasiperiodic attractor (shown in red), respectively. Right: Time series dynamics of the weird quasiperiodic attractor in red. Green line: $x = 0$. Black lines: $x = \pm h$. Parameter setting: $b = 0.80$, $c = 1.00$, and $h = 0.10$ (top); $b = 0.80$, $c = 1.00$, and $h = 0.05$ (middle); and $b = 0.60$, $c = 1.00$, and $h = 0.05$ (bottom). (For interpretation of the references to colour in this figure legend, the reader is referred to the web version of this article.)

analytical results. Proposition 1 characterizes the basins of attraction of the nonfundamental fixed points, while Proposition 2 reveals the types of dynamics our model may produce with respect to the market impact of chartists and fundamentalists.

Proposition 1. For $0 < b < 1$, the basin of attraction of the segment S^* of fixed points consists of an immediate basin $\mathscr{B}_0(S^*)$, and all its preimages of any rank, where $\mathscr{B}_0(S^*)$ is a parallelogram with vertices $(-h, -h)$, $(h, -h + 2h/b)$, (h, h), and $(-h, h - 2h/b)$.

Note that the boundaries of the immediate basin of attraction of the segment S^* of fixed points depend solely on parameters b and h. Why is this the case? Since fundamentalists are inactive when the log of the stock price in deviation from the log of its fundamental value lies between $-h$ and h, the market impact of fundamentalists, represented by parameter c, does not influence $\mathscr{B}_0(S^*)$. However, the size of $\mathscr{B}_0(S^*)$ increases in line with parameter h and decreases in line with parameter b.

We discuss these and some further implications of Proposition 1 using a few examples. The top line of panels of Fig. 7 is based on $b = 0.80$, $c = 1.00$, and $h = 0.10$. The light blue dots in the left panels represent the initial conditions that converge to a nonfundamental fixed point, while the light red dots converge to a weird quasiperiodic attractor, represented in red. While these basins of attraction are identified numerically, we now have analytical insights about the boundaries of the immediate basin of attraction of the segment S^* of fixed points, marked in yellow. The right panel shows the dynamics of the weird quasiperiodic attractor in the time domain.

Suppose policymakers are able to reduce parameter h, for example, by implementing regulations that decrease the risks associated with stock market trading. The middle line of panels of Fig. 7, based on $b = 0.80$, $c = 1.00$, and $h = 0.05$, illustrates the effects of such a policy. Recall that parameter h is a scaling factor. By reducing parameter h from $h = 0.10$ to $h = 0.05$, the magnitude of the fluctuations of the log of the stock price in deviation from the log of its fundamental value associated with the weird quasiperiodic attractor is halved. The same is true for the segment S^* of fixed points, leading to reduced mispricing when the log of the stock price in deviation from the log of its fundamental value converges toward a nonfundamental fixed point, and also its immediate basin of attraction shrinks.

Alternatively, suppose policymakers are able to reduce parameter b, for instance, by implementing regulations that diminish the market impact of chartists. The bottom line of panels of Fig. 7, based on $b = 0.60$, $c = 1.00$ and $h = 0.05$, illustrates the effects of such a policy. As shown, the size of the immediate basin of attraction of the segment S^* of fixed points expands. This policy has no impact on the segment S^* of fixed points, and the magnitude of the fluctuations of the log of the stock price in deviation from the log of its fundamental value remains relatively stable.

Fig. 7 also reveals that the total basin of attraction for the two coexisting attractors changes in a nontrivial way, highlighting the complexity of our model's behavior. We will see more examples of this when we discuss the implications of the following proposition.

Proposition 2. (1) For $b > 1$, all trajectories are divergent except for the segment S^* of saddle fixed points. (2) For $0 < b < 1$ and $c > 2(1 + b)$, the basin of attraction of the segment S^* of fixed points is given by $\mathscr{B}_0(S^*)$ and a sequence of disconnected preimages of any rank of this set via the inverses f_L^{-1} and f_R^{-1}; all other points have divergent trajectories. (3) For $0 < b < 1$ and $c < 2(1 - b)$, the segment S^* of fixed points is globally attracting. (4) For $0 < b < 1$ and $2(1 - b) < c < 2(1 + b)$, weird quasiperiodic attractors may coexist with the attracting segment S^* of fixed points.

According to Proposition 2, there are indeed four parameter regions, see again Fig. 6, that lead to different outcomes. In region R1, given by $0 < b < 1$ and $c < 2(1 - b)$, the market impact of both chartists and fundamentalists is relatively low. As a result, the generic trajectory of the log of the stock price in deviation from the log of its fundamental value converges to a nonfundamental fixed point.[5] In region R2, given by $0 < b < 1$ and $2(1 - b) < c < 2(1 + b)$, the market impact of chartists and fundamentalists is moderate. Consequently, the generic trajectory of the log of the stock price in deviation from the log of its fundamental value either converges to a nonfundamental fixed point or exhibits endogenous dynamics.[6] In region R3, given by $0 < b < 1$ and $c > 2(1 + b)$, the market impact of fundamentalists is relatively high. In this region, the generic trajectory of the log of the stock price in deviation from the log of its fundamental value either converges to a nonfundamental fixed point or displays divergent dynamics. In region R4, given by $b > 1$, the market impact of chartists is relatively high, and the generic trajectory of the log of the stock price in deviation from the log of its fundamental value follows a divergent path.

Figures 8 to 11 provide a selection of examples that further illustrate the dynamics of map M and the implication of Propositions 1 and 2. Figs. 8 and 9 show basins of attraction and time series dynamics for increasing values of parameter c, while keeping parameters b and h equal to $b = 0.80$ and $h = 0.05$. For $c = 0.25$, the generic trajectory of the log of the stock price in deviation from the log of its fundamental value converges to a nonfundamental fixed point located on segment S^*. In fact, the typical behavior in region R1 is that the stock market displays permanent constant mispricing. For c equal to 1.00, 1.70, 2.05, and 2.50, the generic trajectory of the log of the stock price in deviation from the log of its fundamental value either converges to a nonfundamental fixed point or it displays weird quasiperiodic dynamics. All these examples are associated with region R2.

While the basins of attraction that give rise to weird quasiperiodic attractors tend to increase with parameter c, there are exceptions. For instance, at $c = 2.05$, the majority of the initial conditions result in constant mispricing. In addition, the initial conditions that lead to endogenous dynamics produce a weird quasiperiodic attractor that is not symmetric with respect to the origin, revealing the existence of a second weird periodic attractor that is symmetric to it with respect to the origin. See Appendix B for a deeper discussion. At $c = 3.61$, the generic trajectory of the log of the stock price in deviation from the log of its fundamental value either converges to a nonfundamental fixed point or diverges. Once again, note that the immediate basin of attraction of the segment S^* of fixed points is independent of parameter c.

Figures 10 and 11 show basins of attraction and time series dynamics for increasing values of parameter b, while keeping parameters c and h equal to $c = 1.35$ and $h = 0.05$. For $b = 0.30$, the generic trajectory of x_t converges to a nonfundamental fixed point. In region R1, the stock market always displays constant mispricing. For b equal to 0.40, 0.50, 0.60, and 0.80, the generic trajectory of x_t either converges to a nonfundamental fixed point or displays weird quasiperiodic dynamics, as to be expected in region R2. At $b = 1.05$, the stock market is subject to divergent dynamics, except when the initial conditions are located on the segment S^* of fixed points. See part (1) of Proposition 2. The immediate basin of attraction of the segment S^* of fixed points shrinks with parameter b, until it disappears.

4. Stochastic model dynamics

So far, we have examined the deterministic version of our model. In

[5] Only those combinations of x and y that lie on the line $y = x/b$ within the strip between $-h$ and h, as well as their preimages, converge to the origin.

[6] Remarkably, our model predicts that the log of the stock price may oscillate around the log of its fundamental value for parameter combinations that are usually associated with stable dynamics. For the linear chartist-fundamentalist model, i.e., map F, this is not the case. In particular, the green parameter space depicted in the left panel of Figure 1 yields ordinary fixed-point dynamics.

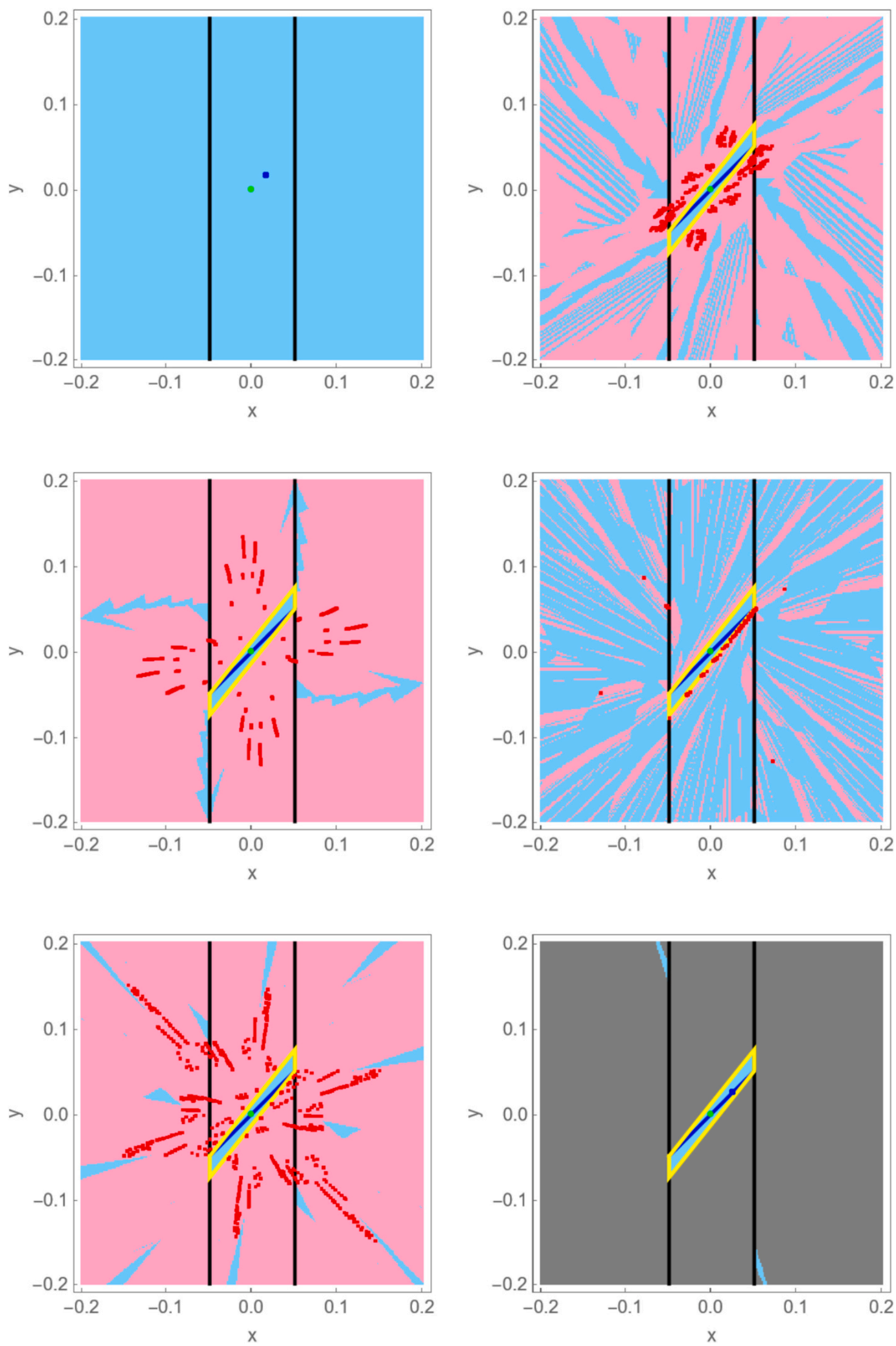

Fig. 8. Basins of attraction for different values of parameter c. From top left to bottom right, parameter c takes the values 0.25, 1.00, 1.70, 2.05, 2.50, and 3.61, while the remaining parameters are set to $b = 0.80$ and $h = 0.05$. The initial conditions from the light blue, light red, and gray area result in fixed-point, weird-quasi-periodic, and divergent dynamics, respectively. Blue dots: fixed point attractors. Red dots: weird-quasiperiodic attractors. Green dots: origin. Blue lines: segment S^* of fixed points. Yellow lines: boundaries of $\mathscr{B}_0(S^*)$. Black lines: $x = \pm h$. (For interpretation of the references to colour in this figure legend, the reader is referred to the web version of this article.)

Section 4.1, we demonstrate that fundamental shocks can lead to intricate attractor-switching dynamics. In Section 4.2, we show that the stochastic version of our model successfully replicates several important stylized facts of stock markets.

4.1. The effects of fundamental shocks

Fig. 12 illustrates examples where the model's dynamics are subject to fundamental shocks. From top to bottom, we set parameter c to 0.45, 0.75, and 1.10, respectively, while the other parameters are fixed at $b = 0.80$, $h = 0.05$, $\sigma_\delta = 0.005$, $\sigma_\chi = 0$, and $\sigma_\phi = 0$. All three parameter constellations fall within region R2. The stochastic behavior of the log of the stock price, expressed in deviations from the log of its fundamental value, is shown in purple. The relations $x = 0$ and $x = \pm h$ are marked in green and black, respectively. The left panels present the dynamics in the time domain and the right panels in state space. Of course, the computations of the basins of attraction displayed in the right panels of Fig. 12 are based on the deterministic version of our stock market model.

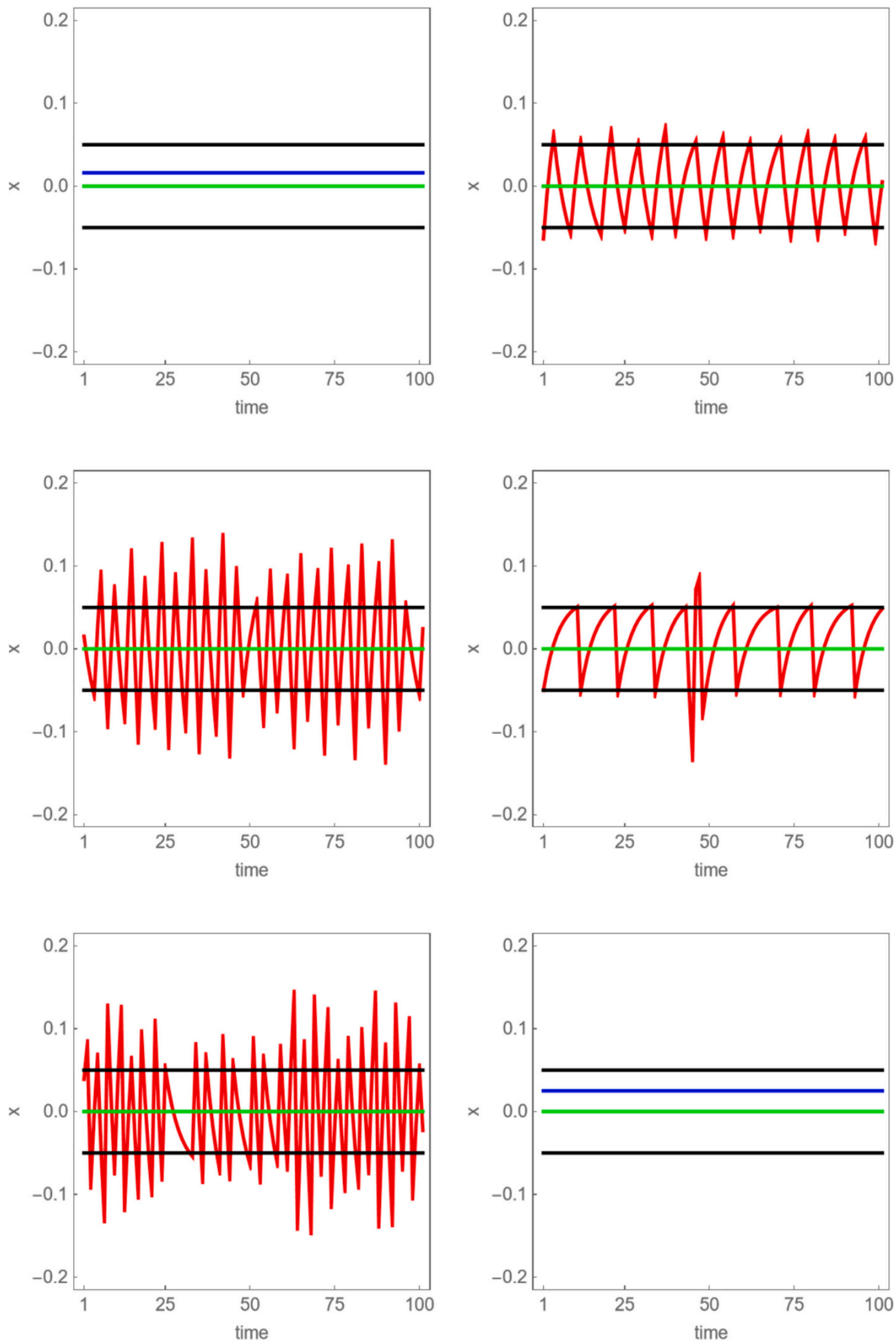

Fig. 9. Dynamics in the time domain for different values of parameter c. The same parameter setting as in Fig. 8. Green line: $x = 0$. Blue line: fixed-point dynamics. Red line: weird-quasiperiodic dynamics. Black lines: $x = \pm h$. (For interpretation of the references to colour in this figure legend, the reader is referred to the web version of this article.)

As can be seen, the log of the stock price in deviation from the log of its fundamental value alternates between the basin of attraction of the segment S^* of fixed points and the basin of attraction of the weird quasiperiodic attractor. We understand the dynamics as follows. When the log of the stock price in deviation from the log of its fundamental value lies within the basin of attraction of the segment S^* of fixed points, the stock market tends to experience mild fluctuations. Due to the fundamental shocks, however, the log of the stock price in deviation from the log of its fundamental value eventually exits this basin. For a time, the stock market then undergoes significant fluctuations until it returns to the previous basin. Importantly, when the log of the stock price in deviation from the log of its fundamental value is in the basin of

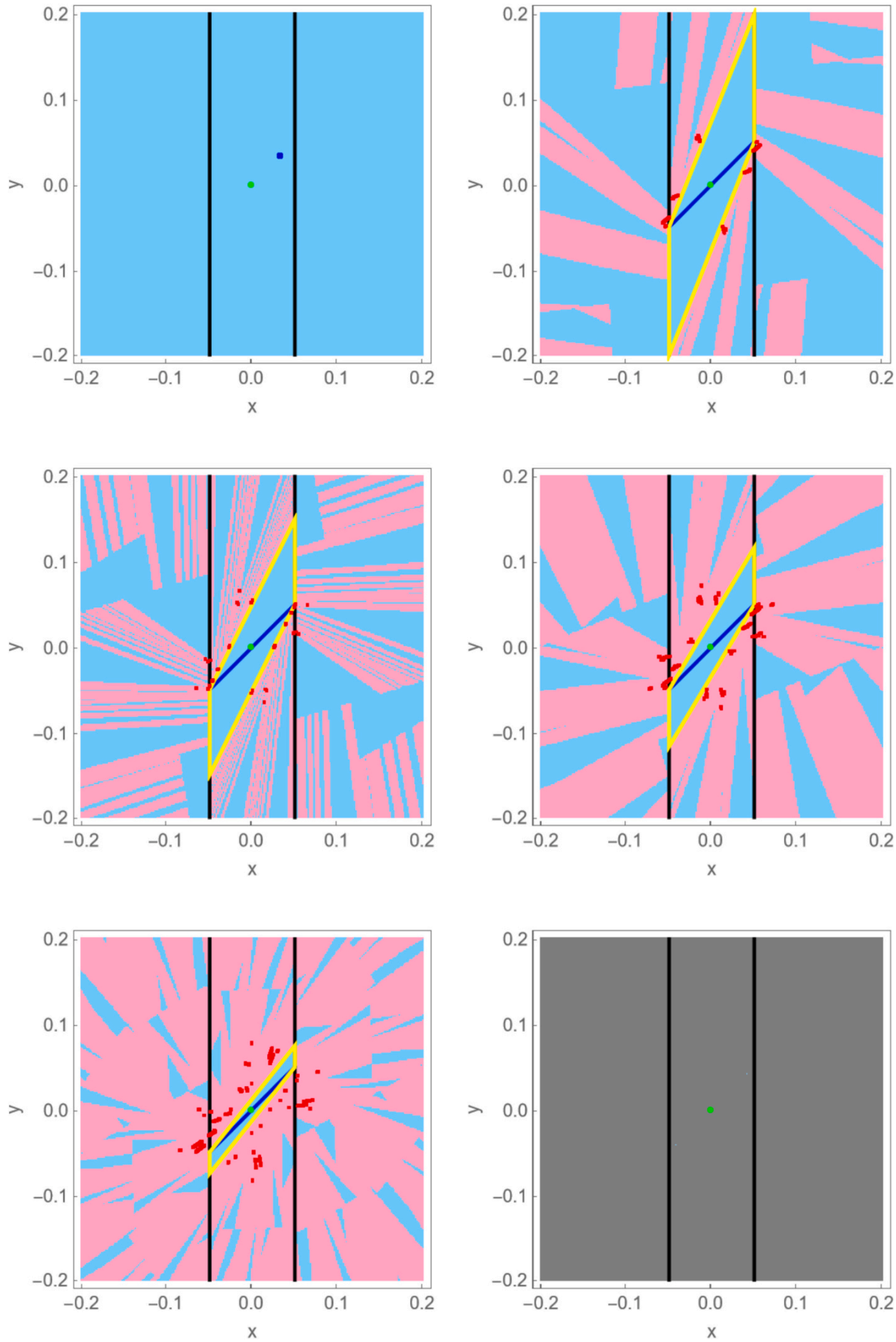

Fig. 10. Basins of attraction for different values of parameter b. From top left to bottom right, parameter b takes the values 0.30, 0.40, 0.50, 0.60, 0.80, and 1.05, while the remaining parameters are set to $c = 1.35$ and $h = 0.05$. The initial conditions from the light blue, light red, and gray area result in fixed-point, weird-quasiperiodic, and divergent dynamics, respectively. Blue dots: fixed point attractors. Red dots: weird-quasiperiodic attractors. Green dots: origin. Blue lines: segment S^* of fixed points. Yellow lines: boundaries of $\mathscr{B}_0(S^*)$. Black lines: $x = \pm h$. (For interpretation of the references to colour in this figure legend, the reader is referred to the web version of this article.)

attraction of the weird quasiperiodic attractor, a substantial part of the stock market's dynamics has an endogenous nature.

Note that the size and structure of the basins of attraction influence the duration of the two regimes and the frequency of regime shifts. For instance, as parameter c increases from 0.45 to 1.10, the total basin of attraction of the weird quasiperiodic attractor expands, making the volatile regime more dominant. Similar dynamics are observed with increasing values of parameter b.

4.2. Matching actual stock market dynamics

Stock prices exhibit several salient statistical properties. Prominent

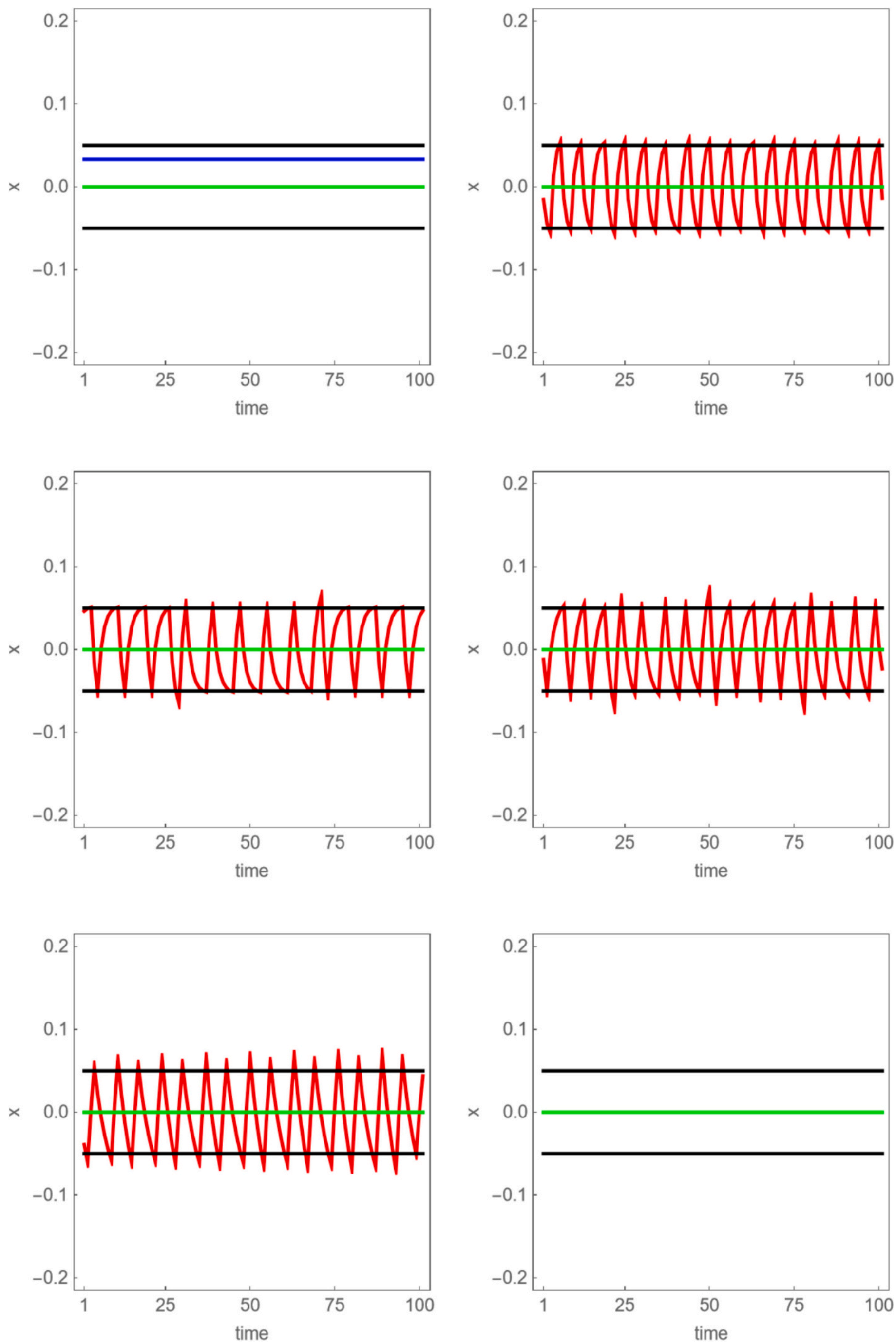

Fig. 11. Dynamics in the time domain for different values of parameter b. The same parameter setting as in Fig. 10. Green line: $x = 0$. Blue line: fixed-point dynamics. Red line: weird-quasiperiodic dynamics. Black lines: $x = \pm h$. (For interpretation of the references to colour in this figure legend, the reader is referred to the web version of this article.)

stylized facts of stock markets include bubbles and crashes, excess volatility, fat-tailed return distributions, serially uncorrelated returns, and volatility clustering. For reviews of these statistical properties, see Mantegna and Stanley (2000), Cont (2001), and Franke and Westerhoff (2012). In the following, we demonstrate that the stochastic version of our model has the potential to generate realistic stock market dynamics. An example based on the parameter setting $b = 0.04$, $c = 0.012$, $h = 0.1$, $\sigma_\delta = 0.002$, $\sigma_\chi = 0.01$, and $\sigma_\phi = 0.03$, is presented in Fig. 13.

- Bubbles and crashes: The black line in the first panel of Fig. 13 shows the stochastic evolution of the stock price, while the gray line represents its fundamental value. Assuming 250 trading periods per

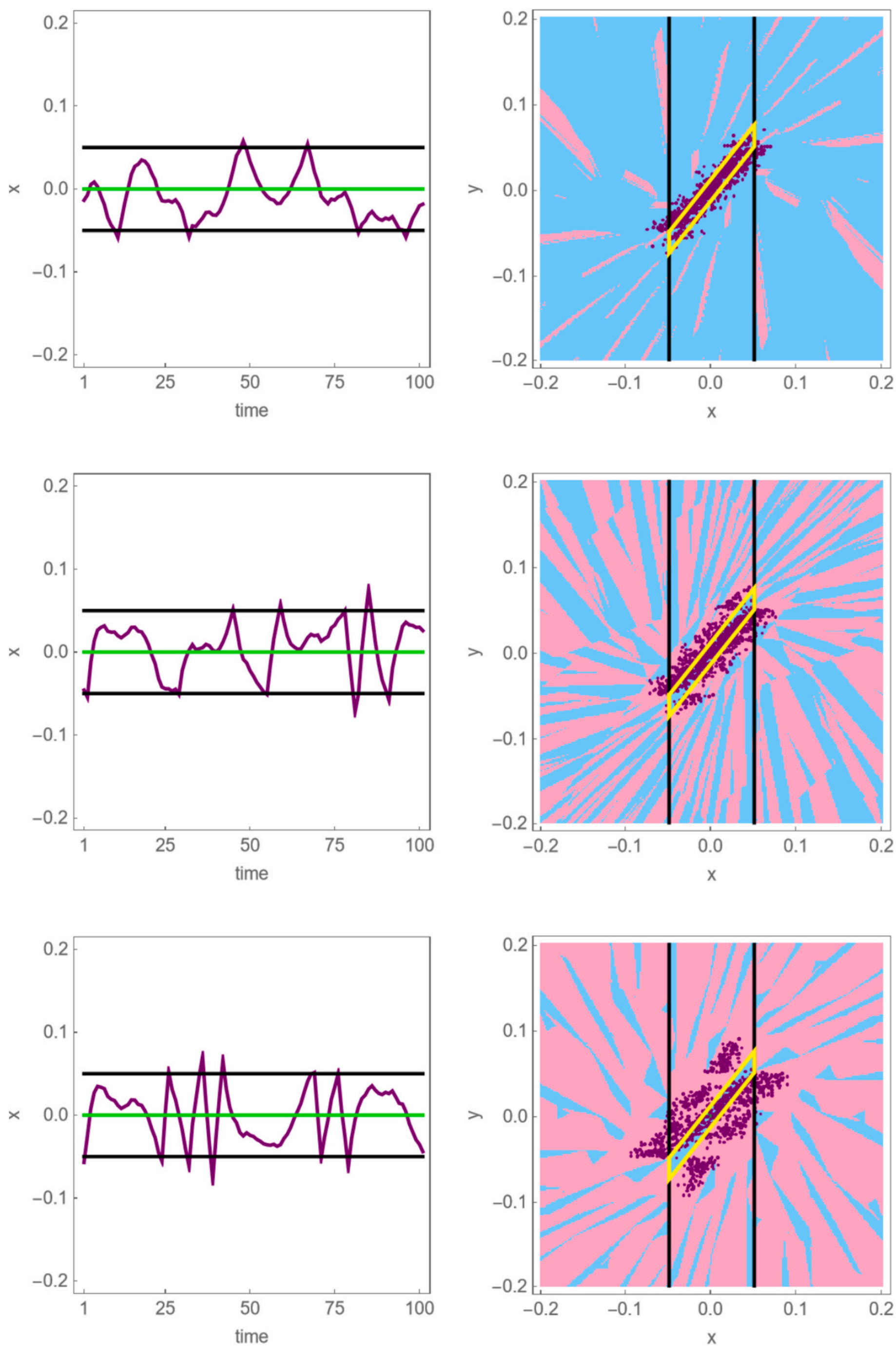

Fig. 12. Stochastic stock market dynamics. The left panels depict the evolution of x_t, $x = 0$, and $x = \pm h$ in purple, green, and black, respectively. The right panels show their behavior in state space. In addition, the right panels indicate the basins of attraction of the segment S^* of fixed points and the weird quasiperiodic attractor in light blue and light red, respectively. The boundaries of $\mathscr{B}_0(S^*)$ are displayed in yellow. From top to bottom, parameter c is set to 0.45, 0.75, and 1.10, respectively, with the parameters $b = 0.80$, $h = 0.05$, $\sigma_\delta = 0.005$, $\sigma_\chi = 0$, and $\sigma_\phi = 0$ held constant. (For interpretation of the references to colour in this figure legend, the reader is referred to the web version of this article.)

year, the simulated 5000 observations correspond to a time span of about 20 years in reality. Although the stock price tracks its fundamental value in the long run, there are notable bubbles and crashes. Also from this perspective, our model reconciles the views of Grossman and Stiglitz (1980) and Farmer and Lo (1999) regarding the limits of informationally efficient stock markets.

- Excess volatility: The second panel of Fig. 13 depicts changes in the log of the stock price (black line) and the log of its fundamental value (gray line). It is evident that the stock price is significantly more volatile than its fundamental value. The stock market's excess volatility is driven by the interactive trading behavior of chartists and fundamentalists. Specifically, volatility is low when mispricing is low, and chartists are the sole type of active speculators. Conversely, volatility is high when mispricing is high, and chartists and fundamentalists are jointly active.
- Fat-tailed return distributions: The third panel of Fig. 13 compares the log distribution of normalized returns generated by the stochastic version of our model with a standard normal distribution. Returns

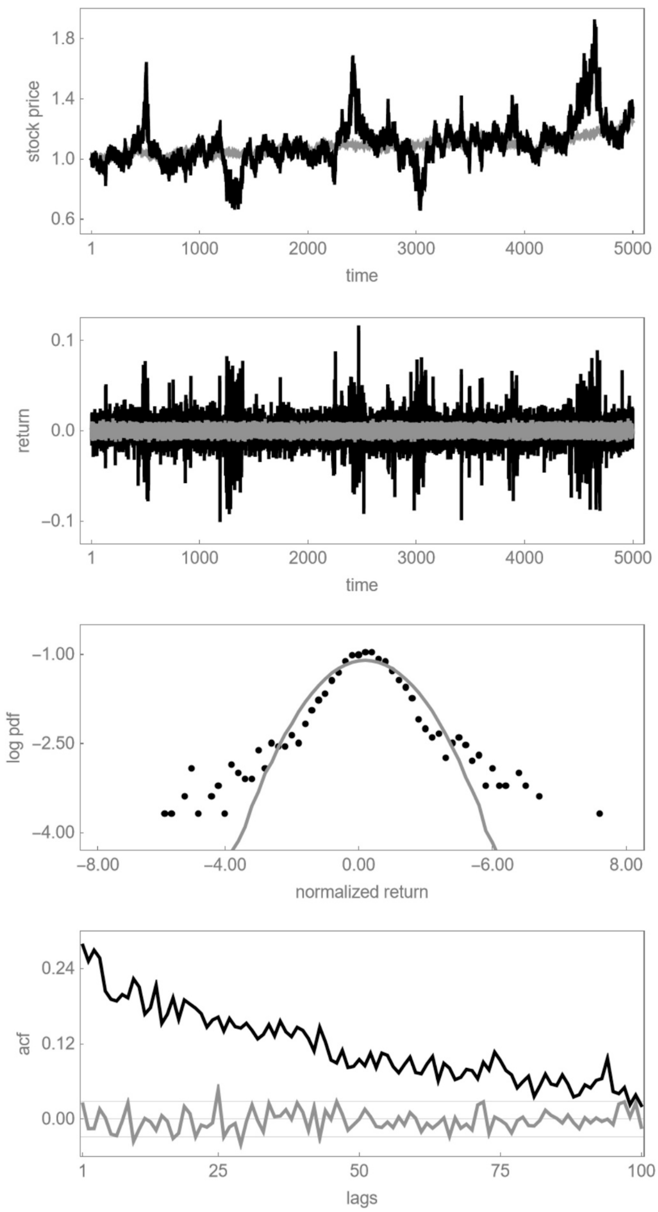

Fig. 13. Matching the stylized facts of stock markets. First panel: Evolution of the stock price (black line) and its fundamental value (gray line). Second panel: Corresponding returns of the stock price (black line) and its fundamental value (gray line). Third panel: Log distribution of normalized returns (black dots) compared to the standard normal distribution (gray line). Fourth panel: Autocorrelation coefficients of raw returns (gray line) and absolute returns (black line) over 100 lags. Parameter setting: $b = 0.04$, $c = 0.012$, $h = 0.1$, $\sigma_\delta = 0.002$, $\sigma_\chi = 0.01$, and $\sigma_\phi = 0.03$.

are normalized by dividing them by their standard deviation. As in reality, simulated returns exhibit more probability mass in the tails of the distribution than a normal distribution with the same mean and standard deviation. Extreme price changes are also evident in the second panel of Fig. 13.

- Random walk and volatility clustering: The fourth panel of Fig. 13 shows the autocorrelation coefficients of raw returns (gray) and absolute returns (black) for 100 lags. Since the raw returns are serially uncorrelated, the stock price path resembles a random walk. As Samuelson (1965) proved, informationally efficient stock prices fluctuate randomly. However, our model suggests that non-informationally efficient stock prices may also fluctuate randomly. In contrast, the autocorrelation coefficients of absolute returns remain highly significant, even up to 100 lags. The volatility clustering behavior of the stock market is also evident in the second panel of Fig. 13.

Since the results presented in Fig. 13 are robust across multiple simulation runs, we can conclude that our stock market model is supported by the data.

5. Conclusions

We examine the extent to which stock markets are informationally efficient using a chartist-fundamentalist model. Fama (1970) argues that stock prices reflect all available information. As demonstrated by Samuelson (1965), stock prices then fluctuate randomly. Grossman and Stiglitz (1980) emphasize that speculators need an incentive to gather, analyze, and act on information, which leads to constant mispricing. According to Farmer and Lo (1999), a stock market's mispricing should be seen as dynamic rather than static, as speculators are boundedly rational and regularly adjust their behavior in response to their market experiences.

Our main results are as follows. First, our model demonstrates the potential for the joint emergence of constant and oscillatory mispricing, reconciling the views of Grossman and Stiglitz (1980) with those of Farmer and Lo (1999). Second, we identify the existence of a weird quasiperiodic attractor – a novel dynamic behavior that blurs the lines between quasiperiodic and chaotic dynamics, thereby deepening our understanding of the complex behavior of stock markets. Third, the stochastic version of our model explains several stylized facts of stock markets, including bubbles and crashes, excess volatility, fat-tailed return distributions, serially uncorrelated returns, and volatility clustering. One might argue that our model is empirically validated – not only is it grounded in observations, but it also generates dynamics closely resembling those of real stock markets. Overall, our findings underscore the importance of considering piecewise-linear discontinuous models in the analysis of economic systems.

Declaration of competing interest

None.

Acknowledgements

Laura Gardini and Davide Radi thank the VŠB-Technical University of Ostrava (SGS Research Project SP2024/047) and the European Union (REFRESH Project – Research Excellence for Region Sustainability and High-Tech Industries of the European Just Transition Fund, Grant CZ.10.03.01/00/22 003/000004). The work of Davide Radi and Iryna Sushko was funded by PRIN 2022 under the Italian Ministry of University and Research (MUR), Prot. 2022JRY7EF – Qnt4Green: Quantitative Approaches for Green Bond Market – Risk Assessment, Agency Problems and Policy Incentives. Davide Radi acknowledges the support of the Czech Science Foundation (GACR) under Project 22-28882S, the VŠB-Technical University of Ostrava under the SGS Project SP2023/019, and the Gruppo Nazionale di Fisica Matematica (GNFM-INdAM).

Appendix A. Proof of Proposition 1

The eigenvalues of the Jacobian matrix J_M, associated with the middle partition of map M, are $\lambda_1 = 1$, with eigenvector $r_1 = (1, 1)$ along the main diagonal, and $\lambda_2 = b$, with eigenvector $r_2 = (1, 1/b)$. It follows that for $0 < b < 1$, the attracting eigenvector originating from each fixed point (u, u) of the segment S^* of fixed points is a segment of the straight line described by the equation $y = u + (x - u)/b$. This segment must belong to the middle partition of map M, i.e., for $-h < x < h$. From the point $(-h, -h)$, only the upper segment exits, corresponding to the line $y = -h + (x + h)/b$, which intersects the discontinuity line $x = h$ at the point $(h, -h + 2h/b)$. This defines the upper boundary of the immediate basin of attraction of the segment S^* of fixed points, denoted by $\mathscr{B}_0(S^*)$. Conversely, from the point (h, h), only the lower segment exits, corresponding to the line $y = h + (x - h)/b$, which intersects the discontinuity line $x = -h$ at the point $(-h, h - 2h/b)$. This defines the lower boundary of $\mathscr{B}_0(S^*)$.

A few comments are in order. The first preimages of the immediate basin of attraction of the segment S^* of fixed points, i.e., $f_L^{-1}(\mathscr{B}_0(S^*))$ and $f_R^{-1}(\mathscr{B}_0(S^*))$, consist of two symmetric triangles, each with a segment on the discontinuity lines $x = -h$ and $x = h$, respectively, via $f_{L/R}^{-1}(u, v) = \left(v, \frac{(1+b-c)v-u}{b}\right)$. From f_L^{-1}, we obtain the vertices of the triangle in the left partition. They are given by

$$f_L^{-1}(-h, -h) = \left(-h, h\frac{c-b}{b}\right) \quad (A)$$

$$f_L^{-1}\left(-h, -h\left(\frac{2}{b}-1\right)\right) = \left(-h\left(\frac{2}{b}-1\right), \frac{h}{b}\left(-1 + (1+b-c)\left(\frac{2}{b}-1\right)\right)\right) \quad (B)$$

$$f_L^{-1}(h(1-2b), -h) = \left(-h, \frac{h}{b}(b+c-2)\right) \quad (C)$$

The triangle in the left partition of map M is the preimage of the triangle of $\mathscr{B}_0(S^*)$ in the region $y < -h$. The triangle in the right partition of map M is the preimage of the triangle of $\mathscr{B}_0(S^*)$ in the region $y > h$. It follows that no point from the external partitions of map M can be mapped in one iteration in the strip of $\mathscr{B}_0(S^*)$ with $-h < y < h$, which includes the segment S^* of fixed points. This portion has no rank-1 preimage.

Figure A1, based on $b = 0.4$, $c = 2.85$, and $h = 0.05$, provides an example. White points converge toward the segment S^* of fixed points, while gray points exhibit divergent dynamics. The left panel highlights the boundaries of the immediate basin of attraction of the segment S^* of fixed points in yellow. The right panel shows that points A, B, and C are mapped to points A', B', and C', respectively.

A.1. Proof of part (1) of Proposition 2

For $b > 1$, the eigenvector originating from each fixed point (u, u) of the segment S^* of fixed points is repelling (local unstable set), and its points exit from the middle partition of map M after a finite number of iterations. Since the dynamics in the external partitions of map M are also expanding, with real or complex conjugate eigenvalues outside the unit circle, the generic trajectory is divergent. The only points with non-divergent trajectories are those on the segment S^* of saddle fixed points, and such points have no rank-1 preimage under $f_{L,R}^{-1}$.

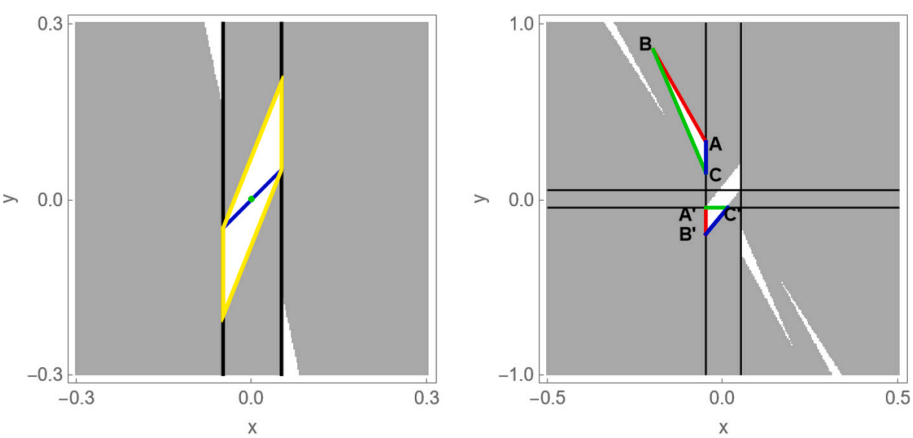

Fig. A1: The basin of attraction of the segment S^* of fixed points. White points converge toward the segment S^* of fixed points, while gray points exhibit divergent dynamics. Parameter setting: $b = 0.40$, $c = 2.85$, and $h = 0.05$.

A.2. Proof of part (2) of Proposition 2

For $0 < b < 1$ and $c > 2(1 + b)$, the two functions $f_{L/R}$ of map M have a virtual saddle fixed point at the origin, with two real negative eigenvalues $\lambda_i = \frac{1}{2}\left((1 + b - c) \pm \sqrt{(1 + b - c)^2 - 4b}\right)$, $i = 1, 2$. The eigenvectors associated with these eigenvalues lie along the lines $y = x/\lambda_i$. Therefore, in the external partitions of map M, points not belonging to the basin of attraction of the segment S^* of fixed points have divergent trajectories.

From the first preimages of $\mathscr{B}_0(S^*)$, specifically $f_L^{-1}(\mathscr{B}_0(S^*))$, point (C), introduced after the proof of Proposition 1, lies above the immediate basin of attraction of the segment S^* of fixed points, as $\frac{h}{b}(b + c - 2) > h$ (which occurs when $c > 2$). Thus, the triangle $f_L^{-1}(\mathscr{B}_0(S^*))$ is disjoint from $\mathscr{B}_0(S^*)$, and the total basin of attraction of the segment S^* of fixed points consists of disconnected elements.∎

A.3. Proof of part (3) of Proposition 2

Let us first assume that the eigenvalues of the Jacobian matrix $J_{L/R}$ are real and positive. In this case, the points in the middle partition of map M that lie outside the immediate basin of attraction of the segment S^* of fixed points have trajectories that enter one of the two external partitions of map

M within a finite number of steps. Points from the external partitions of map M are attracted to the virtual attracting fixed point at the origin, so that any trajectory eventually enters $\mathscr{B}_0(S^*)$ in a finite number of steps.

Before we consider the cases where the eigenvalues of the Jacobian matrix $J_{L/R}$ are real and negative or complex conjugate, note that the boundary $c = 2(1\quad b)$ is related to the geometric shape of the rank-1 preimage of $\mathscr{B}_0(S^*)$ under $f_L^{\ 1}$. The following results hold. The image of $A' = (\quad h,\quad h)$ via f_L lies exactly on the lower boundary of the immediate basin of attraction of the segment S^* of fixed points when $A'' = f_L(\quad h,\quad h) = (\quad h(1\quad c),\quad h)$ lies on the line described by the equation $y = h + (x\quad h)/b$, which occurs only for $c = 2(1\quad b)$.

This means that for $c < 2(1\quad b)$, the point $A'' = f_L(\quad h,\quad h)$ is inside the immediate basin of attraction of the segment S^* of fixed points. Furthermore, a segment of the left boundary of $\mathscr{B}_0(S^*)$ is mapped via both f_L and f_M into the immediate basin of attraction of the segment S^* of fixed points. See the left and middle panels of Fig. A2. In fact, the triangle preimage of the immediate basin of attraction of the segment S^* of fixed points via $f_L^{\ 1}$ includes a segment of $x = \quad h$ that overlaps with $\mathscr{B}_0(S^*)$.

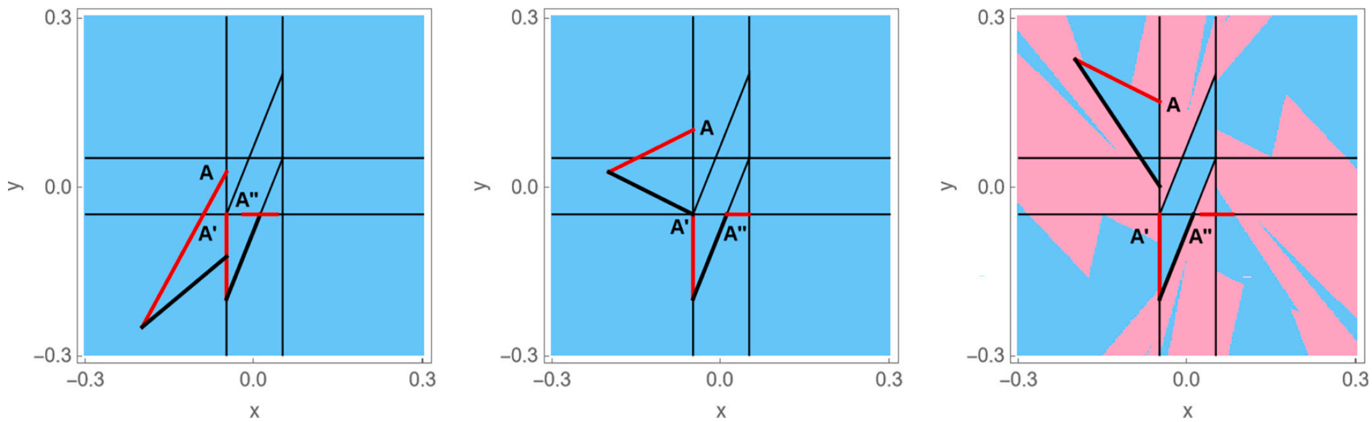

Fig. A2. Basin of attraction of the segment S^* of fixed points. Left: $b = 0.40$, $c = 0.60$, and $h = 0.05$. Center: $b = 0.40$, $c = 1.20$, and $h = 0.05$. Right: $b = 0.40$, $c = 1.60$, and $h = 0.05$.

When the eigenvalues of $J_{L/R}$ are complex conjugate, a point in the external partitions of map M is attracted to the virtual fixed point at the origin, rotating around it with the trajectory of points forming suitable arcs of spirals. A similar behavior also occurs when the eigenvalues of $J_{L/R}$ are real and negative. In this case, points outside the middle partition of map M flip between its left and right partition, with trajectories that tend toward the origin.

In both cases, it follows that within a finite number of iterations, a point of the trajectory will enter $\mathscr{B}_0(S^*)$ or one of its rank-1 symmetric pre-images $f_{L/R}^{\ 1}(\mathscr{B}_0(S^*))$. In other words, since $\mathscr{B}_0(S^*) \cup f_L^{\ 1}(\mathscr{B}_0(S^*)) \cup f_R^{\ 1}(\mathscr{B}_0(S^*))$ forms a connected set, also the total basin of attraction of the segment S^* of fixed points is a connected set, encompassing the entire phase plane. Thus, the segment S^* of fixed points is globally attracting.

A.4. Proof of part (4) of Proposition 1

When $c > 2(1\quad b)$, the point $A'' = f_L(\quad h,\quad h)$ lies outside the immediate basin of attraction of the segment S^* of fixed points (Fig. A.2, right panel). As a result, the rank-1 symmetric preimages $f_{L/R}^{\ 1}(\mathscr{B}_0(S^*))$ are disjoint from $\mathscr{B}_0(S^*)$ and the total basin of attraction of the segment S^* of fixed points may be disconnected. This leads to the possible existence of points with the trajectories that cross all three partitions of map M but never enter $\mathscr{B}_0(S^*)$. Some points of the line $x = \quad h$ between the points C and A' may belong to the basin boundary of a coexisting attractor.

When there exists an attracting set different from the segment S^* of fixed points, numerical evidence shows that the trajectory of $A'' = f_L(\quad h,\quad h)$ converges to that attractor. However, if its trajectory enters $\mathscr{B}_0(S^*)$, then the segment S^* of fixed points is globally attracting.

Recall that divergent trajectories cannot exist in this parameter range. Regarding the structure of the attractor that coexists with the segment S^* of fixed points, consider a cycle of period k with symbolic sequence $\sigma_1 \dots \sigma_k$, where $\sigma_k \in \{L, M, R\}$. Then $M^k(X) = J_k X$, with $J_k = J_{\sigma_k} \dots J_{\sigma_1}$. A periodic point X of the cycle must satisfy the equation $J_k X = X$.

Two cases are possible:

(i) If J_k does not have an eigenvalue of $+1$, then the only solution is $X = 0$, and such a k-cycle cannot exist.

(ii) If J_k has an eigenvalue of $+1$, then it is possible to have k segments filled with fixed points of map M^k (corresponding to points of a k-cycle), which are stable but not attracting for parameters inside the stability region of map F. However, the segments are attracting, since $\det(J_k) = b^k < 1$.

Clearly, case (i) is the generic case. The attracting sets that coexist with S^*, which we call weird quasiperiodic attractor $\mathscr{A}$, have a "weird" geometric shape. These attracting sets cannot include any cycle and are clearly nonchaotic. The latter is due to the fact that in a chaotic set, the unstable cycles are dense and homoclinic, yet there are no cycles in $\mathscr{A}$. For any point X of the attracting set $\mathscr{A}$, $M^n(X) = J_n X$ belongs to the bounded invariant set for any n and point X never becomes periodic, since $J_n X = X$ cannot occur.

Formally, we can characterize the attractor $\mathscr{A}$ coexisting with S^* as follows. Let $\mathscr{B}$ be the total basin of attraction of S^*, and P the complementary set $P = \mathscr{R}^2 \backslash \mathscr{B}$. Then $\mathscr{A} \subseteq \bigcap_{n \geq 0} M^n(P)$. This shows that when $\mathscr{B}$ is not the entire phase plane, another invariant attracting set must exist.∎

Appendix B. Appendix

Due to the symmetry of map M, any existing weird quasiperiodic attractor is either symmetric with respect to the origin, or one more weird quasiperiodic attractor symmetric with respect to the origin exists. Fig. B1 provides an example. The left panel is based on $b = 0.40$, $c = 2.10$, and $h = 0.05$. Light blue points converge to the segment S^* of fixed points, while light red and light brown points converge to the weird quasiperiodic attractors

$\mathscr{A}$ and $-\mathscr{A}$, respectively. The appearance or disappearance of coexisting weird quasiperiodic attractors is associated with contact bifurcations. When two weird quasiperiodic attractors coexist, as a parameter is varied, they can merge due to a contact with their related basins of attraction, leading to a unique weird quasiperiodic attractor. The right panel is based on $b = 0.40$, $c = 2.15$, and $h = 0.05$. After the merging of the two weird quasiperiod attractors, a unique weird quasiperiodic attractor exists

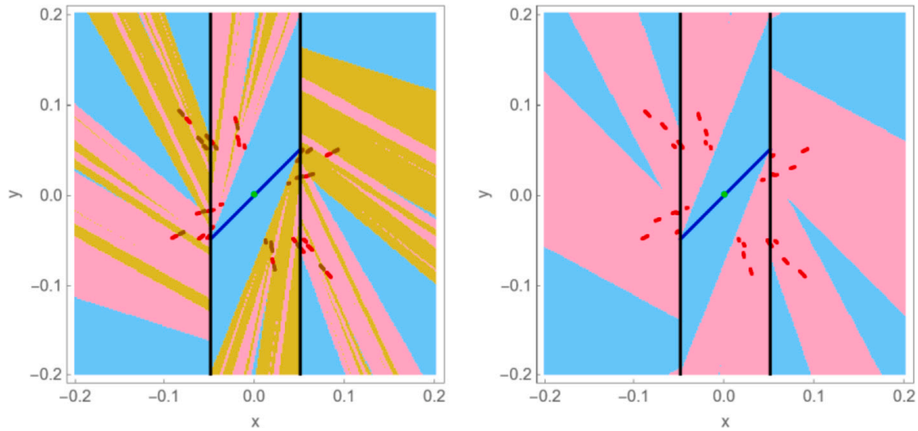

Fig. B1: Appearance and disappearance of coexisting weird quasiperiodic attractors. The left panel is based on $b = 0.40$, $c = 2.10$, and $h = 0.05$. Light blue points converge to the segment of fixed points S^*, while light red and light brown points converge to the weird quasiperiodic attractor $\mathscr{A}$ and $-\mathscr{A}$, respectively. The right panel is based on $b = 0.40$, $c = 2.15$, and $h = 0.05$. Light blue points converge to the segment of fixed points S^*, while light red points converge to the unique weird quasiperiodic attractor $\mathscr{A}$. (For interpretation of the references to colour in this figure legend, the reader is referred to the web version of this article.)

Data availability

No

References

Anufriev, M., Gardini, L., & Radi, D. (2020). Chaos, border collisions and stylized empirical facts in an asset pricing model with heterogeneous agents. *Nonlinear Dynamics, 102*, 993–1017.

Avrutin, V., Gardini, L., Sushko, I., & Tramontana, F. (2019). *Continuous and discontinuous piecewise-smooth one-dimensional maps: Invariant sets and bifurcation structures*. Singapore: World Scientific.

Axtell, R., & Farmer, D. (2025). Agent-based modeling in economics and finance: Past, present, and future. *Journal of Economic Literature, 63*, 197–287.

Beja, A., & Goldman, M. (1980). On the dynamic behavior of prices in disequilibrium. *Journal of Finance, 35*, 235–248.

Bouchaud, J.-P., Farmer, D., & Lillo, F. (2009). How markets slowly digest changes in supply and demand. In T. Hens, & K. R. Schenk-Hoppé (Eds.), *Handbook of financial markets: Dynamics and evolution* (pp. 57–160). North-Holland.

Brock, W., & Hommes, C. (1998). Heterogeneous beliefs and routes to chaos in a simple asset pricing model. *Journal of Economic Dynamics and Control, 22*, 1235–1274.

Cont, R. (2001). Empirical properties of asset returns: Stylized facts and statistical issues. *Quantitative Finance, 1*, 223–236.

Day, R., & Huang, W. (1990). Bulls, bears and market sheep. *Journal of Economic Behavior and Organization, 14*, 299–329.

Di Bernardo, M., Budd, C., Champneys, A., & Kowalczyk, P. (2008). *Piecewise-smooth dynamical systems: Theory and applications*. London: Springer.

Dieci, R., Foroni, I., Gardini, L., & He, X.-Z. (2006). Market mood, adaptive beliefs and asset price dynamics. *Chaos, Solitons and Fractals, 29*, 520–534.

Dieci, R., Gardini, L., & Westerhoff, F. (2022). On the destabilizing nature of capital gains taxes. *International Review of Financial Analysis, 83*, Article 102258.

Dieci, R., & He, X.-Z. (2018). Heterogeneous agent models in finance. In C. Hommes, & B. LeBaron (Eds.), *Handbook of computational economics: Heterogeneous agent modeling* (pp. 257–328). Amsterdam: North-Holland.

Fama, E. (1970). Efficient capital markets: A review of theory and empirical work. *Journal of Finance, 25*, 383–417.

Farmer, D. (2024). *Making sense of chaos*. London: Allen Lane.

Farmer, D., & Lo, A. (1999). Frontiers of finance: Evolution and efficient markets. *Proceedings of the National Academy of Sciences, 96*, 9991–9992.

Feudel, U., Kuznetsov, S., & Pikovsky, A. (2006). *Strange nonchaotic attractors: Dynamics between order and chaos in quasiperiodically forced systems*. Singapore: World Scientific.

Franke, R., & Westerhoff, F. (2012). Structural stochastic volatility in asset pricing dynamics: Estimation and model contest. *Journal of Economic Dynamics and Control, 36*, 1193–1211.

Gardini, L., Radi, D., Schmitt, N., Sushko, I., & Westerhoff, F. (2022). Causes of fragile stock market stability. *Journal of Economic Behavior and Organization, 200*, 483–498.

Gardini, L., Radi, D., Schmitt, N., Sushko, I., & Westerhoff, F. (2023). Sentiment-driven business cycle dynamics: An elementary macroeconomic model with animal spirits. *Journal of Economic Behavior and Organization, 210*, 342–359.

Gardini, L., Radi, D., Schmitt, N., Sushko, I., & Westerhoff, F. (2024). On boom-bust stock market dynamics, animal spirits and the destabilizing nature of temporarily attracting virtual fixed points. *Macroeconomic Dynamics, 29*(e35), 1–31.

Gardini, L., Radi, D., Schmitt, N., Sushko, I., & Westerhoff, F. *On the emergence and properties of weird quasiperiodic attractors*. (2025a). Working Paper, available at: https://arxiv.org/abs/2503.11264.

Gardini, L., Radi, D., Schmitt, N., Sushko, I., & Westerhoff, F. *Abundance of weird quasiperiodic attractors in PWL maps*. (2025b). Working Paper, available at: https://arxiv.org/abs/2504.04778.

Gardini, L., Radi, D., Schmitt, N., Sushko, I., & Westerhoff, F. (2025c). *How risk aversion may shape the dynamics of stock markets: A chartist-fundamentalist approach*. Working Paper. University of Bamberg.

Gardini, L., Sushko, I., & Naimzada, A. (2008). Growing through chaotic intervals. *Journal of Economic Theory, 143*, 541–557.

Graham, B., & Dodd, D. (1951). *Security analysis*. New York: McGraw-Hill.

Grossman, S., & Stiglitz, J. (1980). On the impossibility of informationally efficient markets. *American Economic Review, 70*, 393–408.

Hommes, C. (2011). The heterogeneous expectations hypothesis: Some evidence from the lab. *Journal of Economic Dynamics and Control, 35*, 1–24.

Hommes, C. (2013). *Behavioral rationality and heterogeneous expectations in complex economic systems*. Cambridge: Cambridge University Press.

Hommes, C., Huang, H., & Wang, D. (2005). A robust rational route to randomness in a simple asset pricing model. *Journal of Economic Dynamics and Control, 29*, 1043–1072.

Huang, W., & Day, R. (1993). Chaotically switching bear and bull markets: The derivation of stock price distributions from behavioral rules. In R. Day, & P. Chen (Eds.), *Nonlinear dynamics and evolutionary economics* (pp. 169–182). Oxford: Oxford University Press.

Jungeilges, J., Maklakova, E., & Perevalova, T. (2021). Asset price dynamics in a "bull and bear market". *Structural Change and Economic Dynamics, 56*, 117–128.

Jungeilges, J., Maklakova, E., & Perevalova, T. (2022). Stochastic sensitivity of bull and bear states. *Journal of Economic Interaction and Coordination, 17*, 165–190.

Lillo, F., Farmer, D., & Mantegna, R. (2003). Master curve for price-impact function. *Nature, 421*, 129–130.

Lo, A. (2004). The adaptive markets hypothesis. *Journal of Portfolio Management, 30*, 15–29.

Lux, T. (1995). Herd behaviour, bubbles and crashes. *Economic Journal, 105*, 881–896.

Mantegna, R., & Stanley, E. (2000). *An introduction to econophysics*. Cambridge: Cambridge University Press.

Matsuyama, K. (2007). Credit traps and credit cycles. *American Economic Review, 97*, 503–516.

Matsuyama, K., Sushko, I., & Gardini, L. (2016). Revisiting the model of credit cycles with good and bad projects. *Journal of Economic Theory, 163*, 525–556.

Menkhoff, L., & Taylor, M. (2007). The obstinate passion of foreign exchange professionals: Technical analysis. *Journal of Economic Literature, 45*, 936–972.

Murphy, J. (1999). *Technical analysis of financial markets*. New York: New York Institute of Finance.

Puu, T., & Sushko, I. (2006). *Business cycle dynamics: Models and tools*. New York: Springer.

Samuelson, P. (1965). Proof that properly anticipated prices fluctuate randomly. *Industrial Management Review, 6*, 41–49.

Scholl, M., Calinescu, A., & Farmer, D. (2021). How market ecology explains market malfunction. *Proceedings of the National Academy of Sciences, 118*, Article e2015574118.

Tramontana, F., Westerhoff, F., & Gardini, L. (2010). On the complicated price dynamics of a simple one-dimensional discontinuous financial market model with heterogeneous interacting traders. *Journal of Economic Behavior and Organization, 74*, 187–205.

Tramontana, F., Westerhoff, F., & Gardini, L. (2013). The bull and bear market model of Huang and Day: Some extensions and new results. *Journal of Economic Dynamics and Control, 37*, 2351–2370.

Westerhoff, F. (2012). Interactions between the real economy and the stock market: A simple agent-based approach. *Discrete Dynamics in Nature and Society, 2012*, Article 504840.

Zeeman, E. (1974). On the unstable behaviour of stock exchanges. *Journal of Mathematical Economics, 1*, 39–49.

Zhusubaliyev, Z., & Mosekilde, E. (2003). *Bifurcations and chaos in piecewise-smooth dynamical systems*. New Jersey: World Scientific.